

# DESIGN AND APPLICATION OF SQUEEZE FILM DAMPERS IN ROTATING MACHINERY

by

**Fouad Y. Zeidan**

Director of Engineering

KMC, Incorporated

Houston, Texas

**Luis San Andres**

Associate Professor

and

**John M. Vance**

Professor

Department of Mechanical Engineering

Texas A&M University

College Station, Texas



*Fouad Y. Zeidan is Director of Engineering at KMC, Incorporated, in Houston, Texas. Prior to joining KMC, Dr. Zeidan held positions at Amoco Research Center, IMO Industries CentriMarc Division, and Qatar Fertilizer where he worked in maintenance and troubleshooting of rotating machinery, bearing design and failure analysis, vibration analysis, rotordynamic analysis, upgrading of critical plant equipment, and auditing of new machinery. At KMC, he is working on the design and development of radial and thrust bearings for oil, process, and gas lubricated applications. He has published over 25 technical papers and articles on various turbomachinery topics. He has several patent filings for an integral squeeze film centering spring damper and other high performance journal and thrust bearings. He received his B.S. degree (Mechanical Engineering) (1978), M.S. degree (Mechanical Engineering) (1979), and Ph.D. degree (1989) from Texas A&M University.*



*Luis A. San Andres, Associate Professor of Mechanical Engineering, received his Ms.Sc. from the University of Pittsburgh (1982) and his Ph.D. from Texas A&M University (1985). He has the Applied Science and Technology Award from the Organization of American States (1989), the SAE 1995 Teetor Educational Award, and has been a TEES Fellow since 1993.*

*His research interests are in the areas of fluid film lubrication at high speeds, the mechanics of squeeze film flows, and rotordynamics. Dr. San Andres has contributed extensively to the understanding of fluid inertia effects in thin film squeeze flows and performed experimental work on the measurement of pressure fields on squeeze film damper apparatus typical of jet engine applications.*

*Dr. San Andres' current research interests include the development of sound and efficient computational fluid flow models for prediction of static and dynamic force performance of hydrostatic*

*journal and pad bearings, and annular pressure seals for cryogenic liquid applications. He is also developing a test program to measure the effects of advanced integral squeeze film dampers on rotor-bearing systems.*



*John M. Vance is a Professor of Mechanical Engineering at Texas A&M University. He received his B.S. degree (Mechanical Engineering) (1960), M.S. degree (Mechanical Engineering) (1964), and Ph.D. degree (1967) from the University of Texas.*

*Prior to joining Texas A&M (1978), Dr. Vance held positions at Armco Steel, Texaco Research, and Tracor, Incorporated, and developed a Rotordynamics Laboratory at the University of Florida.*

*Dr. Vance is currently conducting research on rotordynamics, damper seals, and bearing dampers. He published a book entitled Rotordynamics of Turbomachinery (John Wiley, 1988) and more than 50 technical articles and reports. He is consultant to industry and government and has held summer appointments at Pratt and Whitney Aircraft, USARTL (Helicopter Propulsion Lab, Ft. Eustis), Southwest Research Institute, Shell Development Company, and the Center for Electromechanics (University of Texas). He organized the annual short course for industry at Texas A&M on "Rotordynamics of Turbomachinery" and coorganized the biennial "Workshop on Rotordynamics Instability Problems in High Performance Turbomachinery." He serves on the Advisory Committee for the Turbomachinery Symposium. Dr. Vance is a member of ASME and ASEE, and he is a registered Professional Engineer in the State of Texas.*

## ABSTRACT

There are common misconceptions and occasional misapplications associated with squeeze film dampers. The authors have worked for more than 25 years researching, experimenting, and applying this subject matter to all types of turbomachinery. Major strides have been made in advancing the state-of-the-art by

accounting for the fluid inertia effects in the analysis of squeeze film dampers. These effects are very important at high speeds and high temperatures (high squeeze film Reynolds numbers) due to the dominance of the inertial effects in comparison to the viscous effects. A comprehensive discussion is provided of squeeze film dampers, outlining their major advantages and the proper use of these components.

Since squeeze film dampers are more complex to design and analyze than other machinery elements, they have often been used in the process industry as a last resort to reduce vibration or improve the rotordynamic characteristics of a machine. This stigma has often tainted their use as a "band aid" solution and resulted in rejection even when properly applied, with the exception of the aircraft gas turbine industry where their use is widespread. The influence of cavitation in squeeze film damper bearings that is distinctly different than cavitation in journal bearings has only been recently understood. Cavitation, however, is still not amenable to a rigorous quantitative analysis, thus making it essential to rely on experience and knowledge of the applications at hand. It is, therefore, of importance to review the historical events leading to the invention of this device and discuss the major developments in squeeze film dampers to gain a better understanding of the subject matter and an appreciation for the benefits it provides.

## HISTORY OF DEVELOPMENT AND EARLY APPLICATIONS

A report for the U.S Army by Friedericy, et al. [1], shows that design analysis of squeeze film dampers for the Chinook helicopter drive shaft was in progress before 1963. The designs considered were advanced concepts, even by today's standards, consisting of multiple concentric metallic rings around the ball bearing outer race with viscous lubricant supplied to the clearances between the rings. It was found experimentally that the rings had to be pinned against rotation in order to avoid nonsynchronous oil whirl. The Chinook drive shaft is 28 ft long, and so operates through several flexural critical speeds if bearings are not provided at a number of locations along the shaft. The desire to eliminate the weight of these inboard bearings was the incentive for designing squeeze film dampers with frequency dependent damping, so that each critical speed of the supercritical shaft on two bearings would have its optimum damping coefficient. It was shown by analysis that the frequency dependence could be obtained by making the damper rings massive. Unfortunately, the required mass of the damper rings added up to four or five lb, so the frequency dependent characteristic was abandoned. It will be shown that cavitation and air entrainment in the oil would probably have prevented such precise control of the damping coefficients unless a very high lubricant supply pressure was maintained.

A patent application describing a squeeze film damper was filed on November 23, 1966, in the London patent office. The invention was declared by Rolls Royce, Ltd., and the inventor was Arthur Bill. The specification stated: "An advantageous means of damping vibrations in bearings is to provide a hydrodynamic fluid film, sometimes referred to as a "squeeze film," between the bearing and its supporting structure." A U.K. patent number (1,104,478) was assigned and the complete specification was published on November 23, 1968. One of the specific embodiments of the invention was described as an application to axial flow compressor bearings as used in aircraft engines. A significant portion of the specification was devoted to describing means for supplying lubricant to the squeeze film. As shall be shown, lubricant supply conditions are critical in determining squeeze film damper (SFD) performance.

A few years earlier in 1963, a research engineer at Rolls Royce had published a technical paper [2] in which vibration control

experiments on a rotor test rig were described. The results of these experiments are almost certainly the seed of the patent described above, and the reason why squeeze film dampers have been used in most turbojet and turboshaft aircraft engines designed since that time. Squeeze film dampers came to be widely regarded as an essential component of these engines by the 1970s. A turboshaft engineer in the United States explained to the third author in the early 1970s that, even though his company's engines did not have squeeze film dampers designed a priori, the roller bearings actually had a small clearance around the outer race which collected oil and acted as a squeeze film to attenuate vibration.

Cooper's [2] experiments at Rolls Royce were on a 36 in long, 2.0 in diameter shaft, with two 6.0 in diameter wheels spaced 12.5 in apart. Two gas bearings were mounted outboard of the wheels and were suspended on flexible springs to allow the critical speed inversion [3] to take place at low speeds (around 750 rpm). The flexible supports had enough stiffness asymmetry to split the critical speed into two, spaced about 200 rpm apart. Cooper [2] started out using gas bearings, which have very little damping. He found that, although the rotor ran very smoothly at supercritical speeds, the synchronous whirl amplitude when passing through the critical speed was unacceptably large.

Cooper [2] decided to install hard mechanical stops (eight bumpers) around the shaft in an attempt to limit the critical speed amplitude to 3.0 or 4.0 mil. He found that the bumpers prevented inversion and caused violent pounding which threatened the life of the gas bearings. The bumpers were replaced with a concentric metal ring to restrain the shaft and the same pounding and hammering occurred, with delayed (or no) passage through resonance into the smooth "self balanced" mode of operation. The life of the gas bearings was threatened by the violent vibration, so they were replaced with ball bearings in order to accommodate the high loads and abusive testing. The same behavior was observed, except that high frequency vibration was now contributed by the ball dynamics.

After noticing that a hand on the shaft could provide enough damping to smoothly pass through the critical speed, Cooper [2] decided to feed some oil to the clearance between the bumper ring and the shaft and found that the rotor ran smoothly in the inverted mode at very low speeds with the first critical speed not evident. The second critical speed, however, developed into oil whirl. After driving through the oil whirl with severe pounding of the limit ring, inversion was finally obtained with smooth running at high speeds. With regard to this particular test, Cooper [2] states in his paper: "The results were considered worth while and they confirmed the usefulness of proceeding with the less simple scheme which followed." In this following scheme "the hydrodynamic control film was established between nonrotating cylindrical members, a bearing fixed in the structure and a journal which followed the translatory motion of the rotor but was prevented from rotating." The test configuration described in Cooper's [2] paper is shown in Figure 1. One can see that the "bearing" is a large cylinder attached to a fixed frame. The inside diameter has a very wide central oil supply groove. The squeeze film is formed by two lands on each side of the supply groove. The "journal" is the outside diameter of a sleeve that is fitted to the outer race of a ball bearing and supported by coil springs. This configuration has the squeeze film in parallel with the spring supports so that they are subject to the same displacements and share the dynamic load unequally. Most squeeze film dampers in aircraft engines today have a similar arrangement, that is, the "journal" (and roller or ball bearing) are spring-supported with the "bearing" attached to the engine frame as shown in Figure 2 [4]. The squeeze film and the spring support are subject to the same deflection and the dynamic loads are divided unequally between them.

Cooper [2] reported test results for three squeeze film dampers of the Figure 1 configuration, which he referred to as Bearings A,

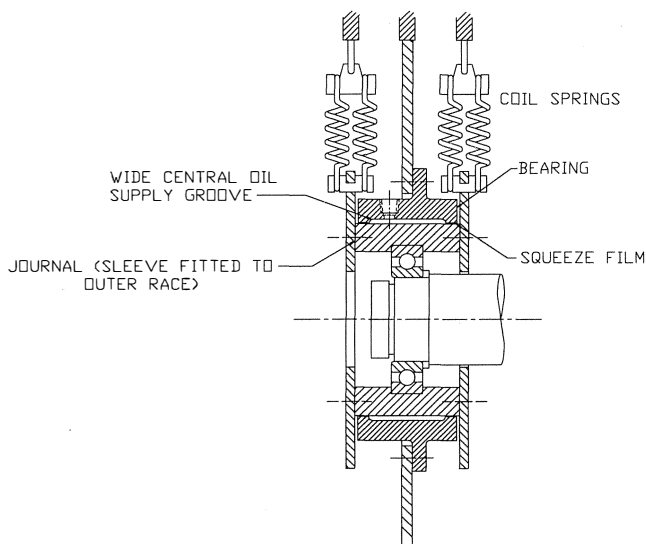


Figure 1. Schematic of Cooper's Squeeze Film Test Apparatus.

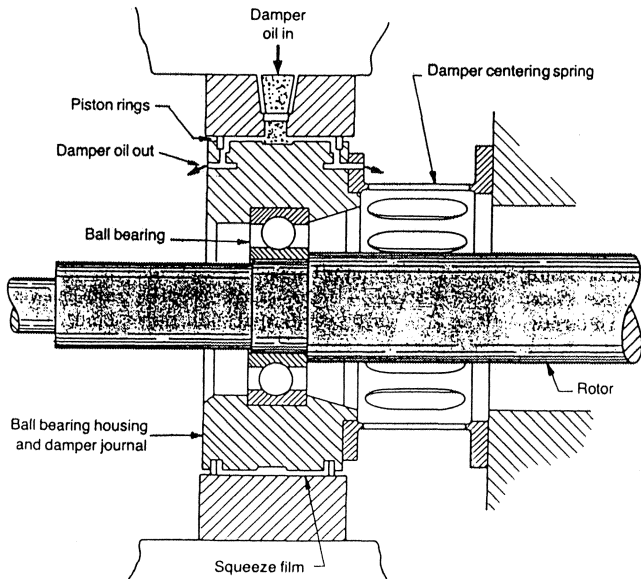


Figure 2. Squeeze Film in Parallel with Squirrel Cage Spring.

B, and C. They had different clearances and land widths. Bearing C, which had the smallest clearance (0.0015 in) had the poorest performance, not allowing inversion at any speed with 0.5 oz/in imbalance. Bearings A and B with 0.003 in clearance performed much better. Bearing A, with the narrowest land (0.1 in), performed best by allowing inversion to a 0.002 in orbit with 1.0 oz/in imbalance. The implication of these results have since been qualitatively confirmed many times over in tests and computer simulations by other researchers. That is, successful SFD designs must have larger clearances than intuition would suggest, and dampers in series with mechanical stiffness have an optimum value of damping which should not be exceeded by making the lands too large. Because of the low speeds of Cooper's tests, he did not discover the various forms of cavitation which have a profound effect on SFD performance at higher speeds.

Cooper [2] also performed a force balance analysis of the whirling bearing which confirmed that inversion can not occur if

the squeeze film land is too wide. The results of his analysis also suggested that, if inversion does occur, three different whirling orbits could exist with force equilibrium: 1) a small orbit with the imbalance inverted to the inside, 2) a large orbit without inversion, and 3) an orbit of intermediate size. Several years later, Cooper's analysis was extended by White [5], a student at the University of Cambridge, who showed that the intermediate orbit is always unstable, that is, the motion will always jump to one of the other orbits. White [5] also showed that the large orbit makes the damper a liability if it persists, but that jumps can occur from the large orbit to the small orbit. This "jump phenomenon," which is a result of the nonlinearity of the squeeze film force, has become the subject of innumerable papers of dubious utility published from academia over the last two decades. A more useful result of White's analysis is that the ratio of imbalance eccentricity to squeeze film clearance must be less than 0.43 in order to maintain the small inverted orbit. Stated another way, the radial clearance must be at least 2.3 times larger than the imbalance for the damper to be effective.

In the early 1970s, squeeze film dampers began to be used to stabilize multistage high pressure centrifugal compressors. The SFD was not a standard component in these machines, but was retrofitted into those machines which exhibited subsynchronous whirl instability. Not all of the retrofits were successful because the required dynamic tuning of the support system was not well understood [6]. This selectivity of application and variable success created a bias against machines fitted with SFD in the industrial user community which persists even today. Nevertheless, a major manufacturer of high pressure centrifugal compressors reports more than 380 machines operating in the field today with squeeze film dampers [7, 8], which is certainly a statement of success.

The traditional application of SFD to industrial compressors is quite different than the typical aircraft application. Aircraft turbine engines all have ball bearings and most are supported on soft "squirrel cage" type supports [3]. The squeeze film journal is a sleeve around the bearing on the free end of the squirrel cage. In contrast, the industrial compressor usually has tilt pad oil film bearings and the squeeze film is installed in series with the tilt pad oil film. A cross section is shown in Figure 3 of the typical configuration [7]. The "oil film" in the figure is the squeeze film. The tilt pad oil film is at the bottom line of the figure (which is also the top surface of the shaft journal). The central groove supplies oil to both the squeeze film and the tilt pad. Two O-rings can be seen in the figure, which often serve a dual purpose: 1) as end seals to restrict leakage of oil from the squeeze film, and 2) as a spring support to center the tilt pad housing and prevent bottoming under the weight of the housing and rotor. Obviously, there is a limit to how much weight a rubber O-ring can support without too much deformation, so this becomes one of the design problems to be solved. The other major design problem is to size the squeeze film dimensions and clearance, and the O-ring properties, for optimum damping and stiffness in series with the tilt pad oil film. This is the problem that Cooper's early experiments exposed, when he found that the SFD with the widest land was the least effective.

## THEORY OF OPERATION AND PRACTICAL LIMITATIONS

The most commonly recurring problems in rotordynamics are excessive steady state synchronous vibration levels, and subsynchronous rotor instabilities. The first problem may be reduced by improved balancing, or by introducing modifications into the rotor-bearing system to move the system critical speeds out of the operating range, or by introducing external damping to limit peak amplitudes at traversed critical speeds. Subsynchronous rotor instabilities may be avoided by eliminating the instability mechanism, or by raising the natural frequency of the rotor-bearing system as high as possible, or by introducing damping to raise the

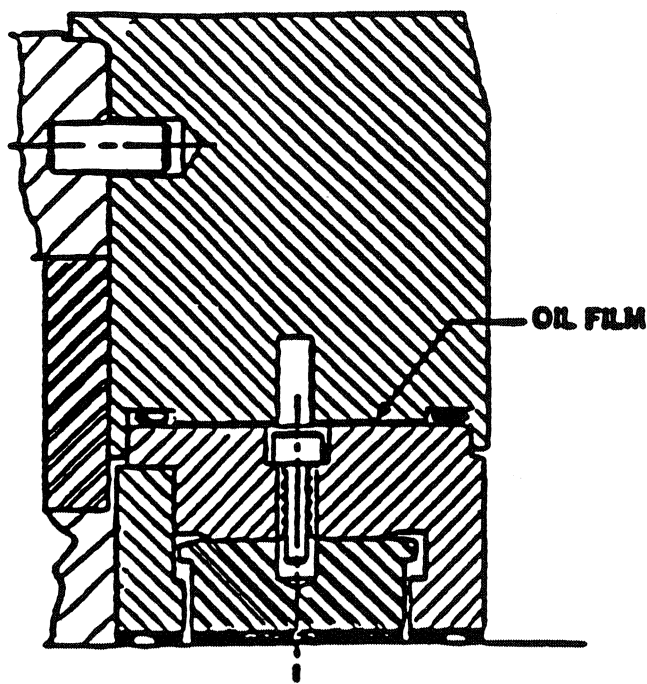


Figure 3. Typical Squeeze Film Configuration in an Industrial Compressor.

onset speed of instability above the operating speed range. The dynamic response of a laboratory shaft and disk supported on a squeeze film damper is shown in Figure 4. The rotor is operating at its natural frequency (36 Hz) and a sudden imbalance is induced on the disk. The top of the figure shows the response of the system without a damper, while the bottom of the figure displays the response with a squeeze film damper. The test results show dramatically the benefits of the damper on the system response.

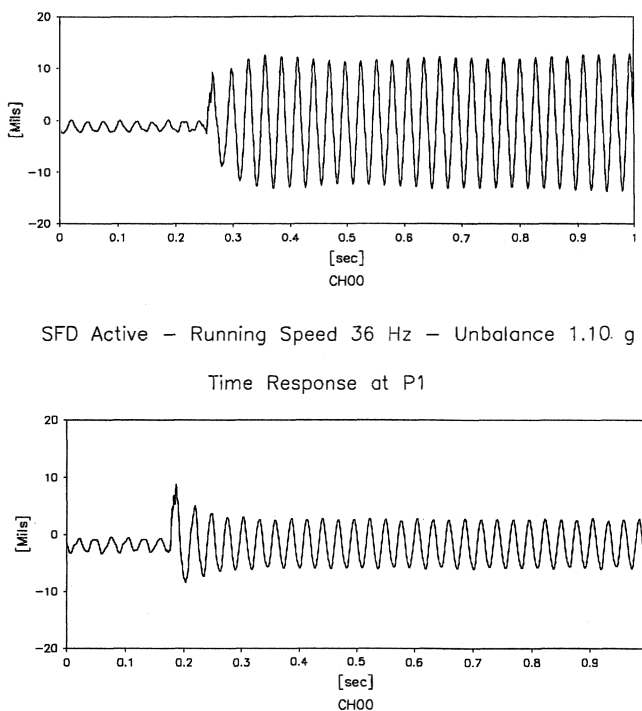


Figure 4. Sudden Unbalance Response of a Laboratory Rotor Supported on Squeeze Film Damper.

Widely varying test results in industry have shown that the design of SFDs is based on overly simplified theoretical models which either fail to incorporate or simply neglect unique features (structural and fluidic) that affect greatly the damper dynamic force performance. The lack of adequate understanding of the mechanics of squeeze film flows is essentially due to the near absence of fundamental experimental evidence and sound rationale that directly addresses the issues and problems of interest. Squeeze film dampers in certain regimes of operation can also bring strong nonlinearities to the performance of rotor-bearing systems. There have been just a few experimental investigations addressing the nonlinear complex interaction between the flow mechanics in squeeze film dampers and the dynamics of the rotor-bearing system.

In its most simple form, a squeeze film damper consists of an inner nonrotating journal and a stationary outer bearing, both of nearly identical radius. An idealized schematic is shown in Figure 5 of this type of fluid film bearing. The journal is mounted on the external race of the rolling element bearing and prevented from spinning with loose pins or a squirrel cage, which provides a centering spring mechanism. The annular gap between the journal and housing is filled with some type of lubricant provided as a splash from the roller bearing lubrication or by a pressurized delivery. In operation, as the journal moves due to dynamic forces acting on the system, the fluid is displaced to accommodate these motions. As a result, generated hydrodynamic pressures exert fluid film forces on the journal surface and provide for a mechanism to attenuate transmitted forces and reduce the rotor amplitude of motion. The amount of damping produced is the critical design consideration. If damping is too large, the SFD acts as a rigid constraint to the rotor-bearing system with large forces transmitted to the supporting structure. If damping is too light, the damper is ineffective and likely to permit large amplitude motions with possible subsynchronous frequencies.

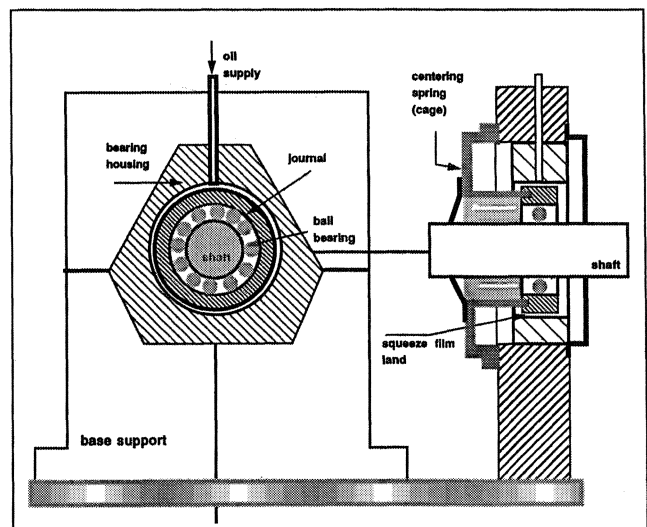


Figure 5. Schematic View of a Squeeze Film Damper.

The performance of squeeze film dampers is not only determined solely by their geometry (length, diameter, and radial clearance) and the viscosity of the lubricant used, but affected greatly by a number of specific design and operating conditions. The level of supply pressure, the feeding and discharge flow mechanisms, the type of end seals, fluid inertia, and dynamic cavitation are but a few of these important factors.

### Influence of End Seals

SFDs are usually designed to incorporate some type of end seals to reduce the axial through flow and increase the damping coefficients [3]. Three common end seal configurations are shown in Figure 6 incorporating piston-rings or elastomeric rings. Jung, et al. [9], and Arauz and San Andres [10] have presented measurements for the pressure field and forces in dampers with open-ends and piston-ring seals. In general, larger damping forces have been measured for the sealed condition although higher fluid thermal rises (accompanied by lower lubricant viscosity) are also a consequence of the sealing devices. Unfortunately, knowledge of the end leakage vs axial pressure drop relationship is required for accurate prediction of the available damping forces. In most circumstances, this is not known and only experience indicates the best type of sealing to be implemented.

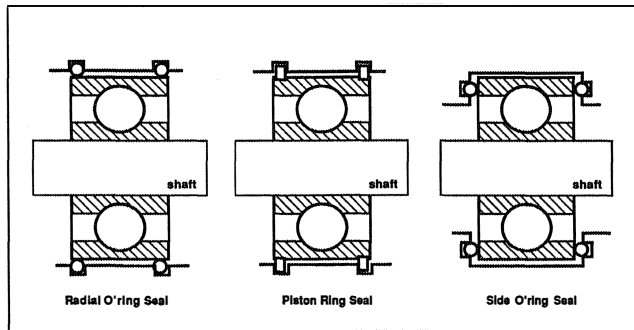


Figure 6. Three Typical End Seal Configurations for Squeeze Film Dampers.

### Effect of feeding circumferential grooves

In many practical circumstances, dampers are designed with a feeding central groove to ensure a continuous flow of lubricant through the squeeze film lands, or with end grooves that act as a plenum before the end seals. The groove, usually of large volume, is thought to provide a uniform flow source or sink with constant pressure around the journal surface. For the central feeding groove-SFD configuration, it is well known theoretically that the level of force obtained is one-fourth that available for a damper with twice the land length. In practice, however, grooved-dampers have been observed to perform much better than current theoretical predictions [11]. Large dynamic pressures have been measured at the groove regions connecting the two squeeze film regions as reported by San Andres, et al. [12], and also Zeidan, et al. [13]. Roberts, et al. [14,15], Ramli, et al. [16], and Rouch [17], have presented experimental force coefficients for a grooved squeeze film damper which are, for all tested journal eccentricities, an order of magnitude larger than predictions from the short bearing model. It is clear then that central grooves in dampers do not isolate the adjacent film lands, but rather interact with the squeeze film regions and generate an appreciable dynamic pressure and force response. Current heuristic explanations for the dynamic effect observed at grooved dampers have referred to fluid inertia and turbulence effects, geometric discontinuities, fluid compressibility, or a combination of all these factors, as the primary sources for the occurrence of the phenomena. Experiments and analysis carried out by San Andres [18] and Arauz, et al. [19, 20], have elucidated the complex flow interactions between feeding groove volumes and the squeeze film lands. The experiments showed measured pressure fields at deep grooves and film lands to be of the same order of magnitude, and where the groove contributed greatly to the overall damping force performance of the damper. For dampers

without lubricant cavitation, the experimental measurements correlated favorably with predictions from this new model and brought to question the typical assumptions leading to the conventional theory of squeeze film flows.

### Fluid Inertia Effects

The importance of fluid inertia in the performance of squeeze film dampers has been demonstrated by numerous theoretical and experimental investigations. The relevance of fluid inertia is related to the squeeze film Reynolds number ( $Re_s = \rho\omega c^2/\mu$ ) which ranges from 1.0 to 50 in many practical applications, notably those related to aircraft jet engines. Theoretical advances on the modelling of high speed dampers have been made by Tichy, et al. [21], and San Andres and Vance [22, 23, 24]. Experimental works relevant to the understanding of SFD performance with fluid inertia effects are given by Vance, et al. [25], Tichy [26], San Andres, et al. [12, 27, 28], Ramli and Roberts [16], Roberts, et al. [14, 15], Kinsali and Tichy [29], Jung, et al. [9], and Zhang, et al. [30]. Some of these experimental works intended to address directly the effect of fluid inertia, while others were interested in the identification of the damper dynamic force characteristics by special methods. Correlation of experimental measurements with analytical predictions, including fluid inertia effects, have ranged from poor to adequate. In general, measured results seem to be highly dependent on actual operating conditions, test hardware configuration, and coupling to the dynamics of the structural system.

### Cavitation Effects

Performance prediction of squeeze film dampers depends on the extent and type of cavitation taking place within the squeeze film land. There have been several experimental investigations which were intended to probe the phenomenon of cavitation in squeeze film dampers and provide some insight, answers, and possible explanations for some of the measurements and behavior which are generally not predicted by the classical lubrication theory. High speed photography was utilized to verify the occurrence of vapor cavitation, along with that of gaseous cavitation which later developed into a two phase mixture of oil and air when the test damper was operated at higher speeds [31, 13, 32, 33].

SFDs in practice operate with low levels of external pressurization which generally do not prevent the lubricant in the fluid film lands from liquid vaporization or entrainment of external gaseous media into the film lands. Investigations of lubricant cavitation in squeeze film dampers has been mostly experimental with results showing a complex phenomena with a profound impact on the forced performance of the dampers tested [34, 35, 36]. Hibner and Bansal [37] showed first that under the influence of fluid cavitation, the pressure fields and fluid film forces were of a unique character and did not correlate well with predictions made using classical lubrication theory. Walton, et al. [34], found that fluid cavitation onset and extent depend on the damper operating parameters like whirl frequency, journal orbit size and eccentricity position, level of supply pressure, and end seal restrictions. Zeidan and Vance [31, 13, 32, 33] have identified five regimes of cavitation in a SFD according to the operating conditions. The experiments demonstrated that air entrance produces gaseous cavitation which under certain conditions determines a nonlinear forced response akin to that of a soft spring. On the other hand, vapor cavitation was shown to lead to a characteristic nonlinear hardening effect. Sun, et al. [35, 36], discuss the major differences between dynamic gaseous and vapor cavitation and the likelihood of their existence in a typical practical application. The significance of these experimental investigations cannot be overlooked, since they have already prompted significant changes in the current philosophy of damper design.

Extensive work and research has been performed on the cavitation phenomenon in steadily loaded journal bearings, and their performance can be accurately predicted. On the other hand, cavitation behavior in dynamically loaded journal bearings is not complete yet, and that in squeeze film dampers lags even further behind. The basic assumption utilized in predicting the performance of dynamically loaded journal bearings and squeeze film damper bearings is that the lubricant film has a similar behavior to that in steadily loaded journal bearings. This implies that the region of cavitation rotates around the journal with the pressure wave, and that the cavitation boundary conditions from steadily loaded journal bearings can be directly applied to dynamically loaded journal bearings and squeeze film damper bearings. White [5] was the first to provide experimental evidence that refuted this assumption. He reported cavitation bubbles that persisted as the journal traversed the high pressure region when operating at journal eccentricities larger than 0.3. Hibner and Bansal [37] showed significant deviation in their measurements from predictions of the theory as the cavitation extent in the damper increased. They hypothesized that the deviation was due to fluid compressibility caused by subatmospheric cavitation pressures liberating dissolved gases and creating a two phase fluid. More recently, Feng and Hahn [38] provided density and viscosity models for two phase homogeneous fluids. While verification of these models is not complete, they point out the inadequacy of the incompressible Reynolds equation in predicting the performance of dynamically loaded bearings and squeeze film dampers operating at high speeds in cavitated conditions.

Investigators working with cavitation in journal bearings and dynamically loaded bearings are mostly concerned with gaseous type cavitation, since these bearings normally operate in a ventilated condition with no end seals. In journal bearings, the oil is drawn into the high pressure region of the film by viscous shear at the surface of the spinning journal. Very little supply pressure is needed to introduce oil into the typical journal bearing. On the other hand, squeeze film dampers normally have some type of end seals, and oil must be supplied to the bearing with some pressure, which normally ranges from a few psig to 60 or 80 psig. The presence of end seals also delays the onset of gaseous cavitation leading to a different type of cavitation normally referred to as vapor cavitation. A trace for the dynamic pressure in the squeeze film is depicted in Figure 7 while operating under vapor cavitation conditions. Note the spike in pressure as the bubble collapses, resulting in an instantaneous increase in pressure and an overshoot in the pressure signal. On the other hand, the trace for the pressure when the damper is operating under gaseous type cavitation shows a distinctively different profile. The positive pressure region is smaller in its circumferential extent and lower in magnitude due to the compressibility of the oil-air mixture. The damping available from the damper under these conditions can be as low as 25 percent of the theoretically predicted value based on the Reynolds lubrication theory.

By virtue of their design and end conditions, squeeze film damper bearings are prone to both types of cavitation; vapor and gaseous. Gaseous cavitation drastically reduces the dynamic load capacity of the damper. At higher speeds and pressures, the gaseous cavities split into smaller cavities leading to the formation of a homogeneous mixture of air and oil. At the same time, large cavities of air continue to form separately from the oil-air mixture, shrinking in size but persisting in the high pressure region.

The assumption of a homogeneous incompressible fluid in the analysis of squeeze film dampers is grossly in error. While the treatment of cavitation in a damper as a  $\pi$ -film model can adequately account for vapor cavitation, it fails in the case of gaseous cavitation. The properties of the homogeneous mixture of oil and air must be incorporated in a compressible fluid model that will also take

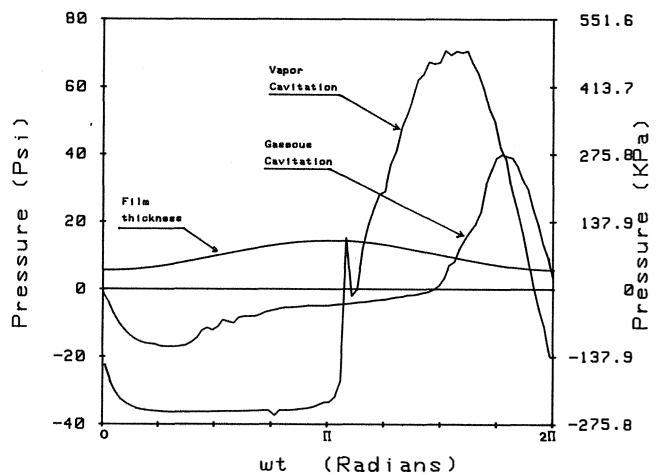


Figure 7. Pressure Profiles in a Squeeze Film Damper Undergoing Vapor and Gaseous Cavitation.

account of the compressibility of the separate patches of air cavities to arrive at a more realistic model that will adequately predict the performance of squeeze film damper bearings.

#### NONLINEARITIES IN SQUEEZE FILM DAMPERS

In the dynamic analysis of rotor-bearing systems, SFDs are regarded as highly nonlinear mechanical elements providing forces obtained from relationships based on the instantaneous journal center eccentricity. Current analysis of rotor-disk assemblies supported on SFDs are based on overly simplified analytical expressions for fluid film forces as derived from the short journal bearing model with the so called  $\pi$ -film cavitation assumption [39, 40, 41].

##### The Jump Phenomenon

The jump phenomenon finds its roots in the stiffness theory of nonlinear oscillations. In particular, systems with a cubic nonlinearity exhibit a response that is characterized by multivaluedness. It is the multivaluedness of the response curve that leads to the jump shown in Figure 8 for a hardening spring. The frequency response shown in the figure is for a single degree of freedom system with a cubic nonlinearity in the stiffness term. As the frequency of excitation is varied, the harmonic response will increase as shown in the following precession 1-2-3-4-5. A jump down in amplitude occurs from 3 to 4, and this characteristic is predicted to take place in a squeeze film damper due to nonlinearity of the crosscoupled damping (stiffness term). This nonlinear response (jump down while accelerating through resonance) have not been experienced in field installations. The senior author observed such a response on an experimental test rig, as shown in Figure 9. The response shows a hardening spring effect while the test rotor was accelerated through the critical speed. However, this hardening effect was not due to the squeeze film stiffness but due to journal lockup that produced a moment stiffness similar to what happens with gear coupling when they lockup.

Computational predictions based on direct numerical integration, and lately analytical solutions based on current nonlinear dynamics models with elegant mathematical methods, show that the forced response of rotor SFDs systems is highly nonlinear with extreme sensitivity to imbalance levels. Little effort has been placed on finding a combination of operating and design parameters which will avoid the damper undesirable response. On the other hand, the richness of the nonlinear (theoretical) behavior has been exploited to prove beyond practical limits the amazing accuracy of the nonlinear dynamics models. It is, however, noted

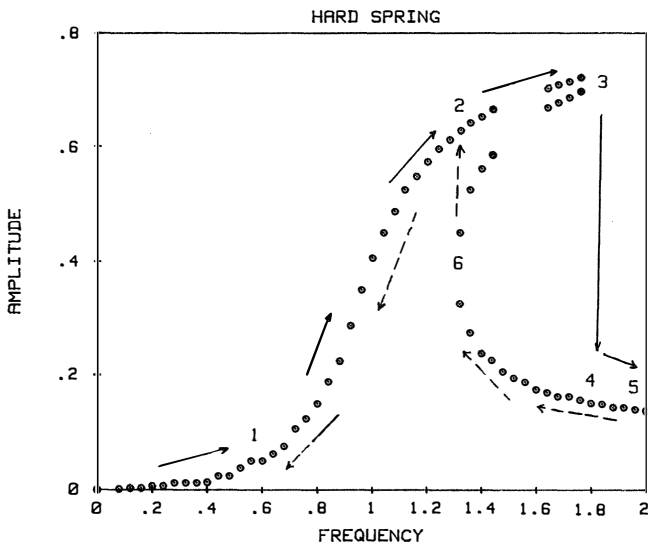


Figure 8. Response of a Nonlinear Hardening Spring.

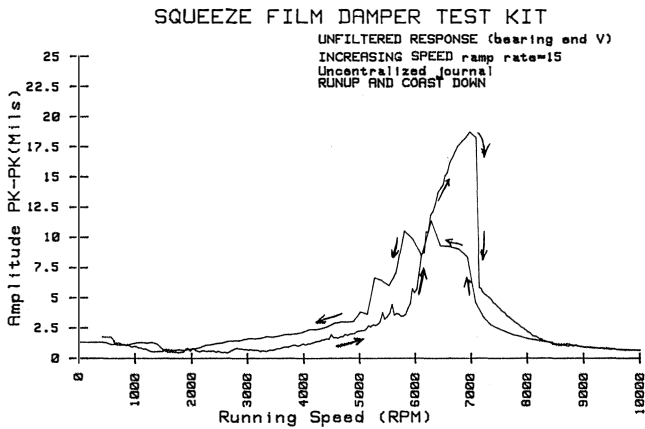


Figure 9. Experimental Measurement of a Jump Down While Accelerating Through the Critical Speed.

that there is little physical evidence and practical experience attesting to the veracity of the theoretical predictions. In the last years, over 20 technical publications have presented extensive theoretical nonlinear dynamics treatments of the problem, and only one publication has investigated the phenomenon by experimental means. No analytical work has provided a sound set of conditions (of practical value) for the development of an experiment directed to validate (or disprove) the theoretical findings. Zhao, et al. [42], provides fundamental experimental evidence showing that current theoretical models fail to predict with accuracy the performance of actual rotor-damper hardware. Zhao, et al. [42], found that the  $\pi$ -film model is unable to correlate with measurements which showed a larger level of damping than expected. In brief, the test rotor-damper system demonstrated a complete absence of jump phenomena and aperiodic forced responses. However, Zhao, et al. [42], failed to understand the nature of the flow in SFDs and stretched the limits of application of the conventional models. As quoted from their work, "the theoretical model need to be used with cavitation pressures as low as  $-700$  KPa ( $-87$  psi) absolute to provide some correlation with the measurements." This assumption allows the lubricant to sustain large levels of tension in an open ends damper configuration. Zeidan, et al. [31, 13, 32], and Sun [36], showed that entrained air is the most likely form of

cavitation in open ended dampers, and thus, lubricant pressures below ambient conditions are (physically) unlikely to occur.

*Bilinear Spring Nonlinearity*

Squeeze film dampers operating without a centering spring and centering spring dampers operating with a high unbalance may experience a bilinear spring effect as shown schematically in Figure 10. The higher stiffness results from the damper journal bottoming out and contacting the higher stiffness housing. This bilinear spring characteristic may lead to nonlinear response often characterized by excitation of the first critical speed or resonance of the structure. Subharmonic response at exact fractions may also be exhibited under these conditions as shown in Figure 11 for a damper without a centralizing spring. A cascade spectrum is shown in Figure 12 for a damper with a centralizing spring experiencing a high unbalance. At certain speeds, the damper journal will impact the housing and excite the first critical speed, while at other instances depending on the ratio of the running speed to the first critical may result in subharmonic vibrations at  $1/2$  or  $1/4$ ,  $2/4$ ,  $3/4$ , or  $1/5$ ,  $2/5$ ,  $3/5$ ,  $4/5$ . In addition to the subharmonic activity, superharmonic vibrations at exact fractions are also evident due to this bilinear spring effect (Figure 13).

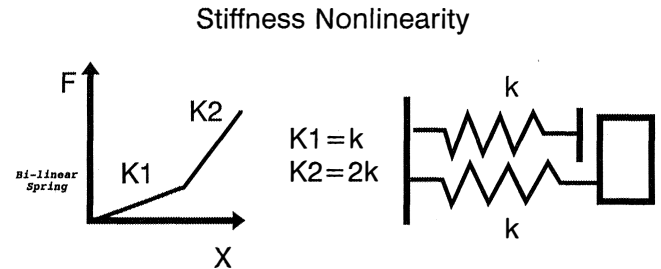


Figure 10. Schematic of a Bilinear Spring.

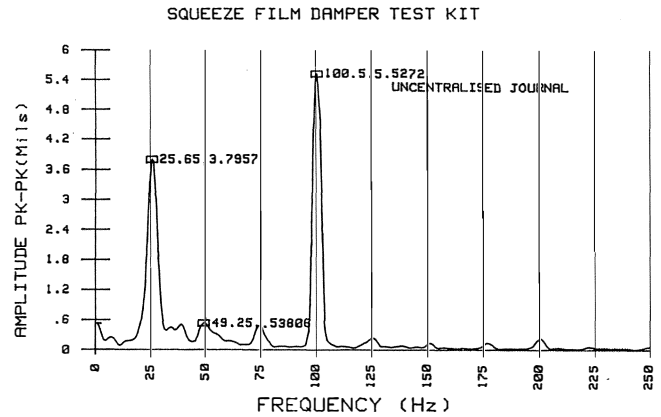


Figure 11. A Frequency Spectrum Showing Subharmonic Vibrations.

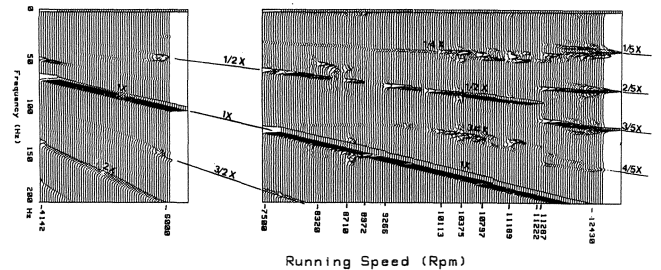


Figure 12. A Cascade Plot for a Damper Showing Regions of Subharmonic Vibrations.

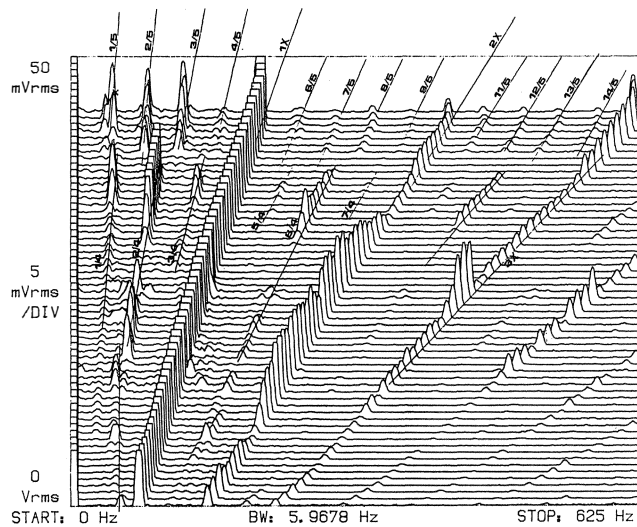


Figure 13. A Frequency Spectrum Showing Subharmonic and Superharmonic Vibrations.

#### Nonlinearity Due to Cavitation

The presence of cavitation and the two phase mixture of oil and air in dampers may cause a loss of damping and contact between the damper journal and the housing that can result in nonlinear response, as shown previously. The response orbit for a damper operating with the same unbalance, but with a different level of pressurization, is shown in Figure 14. Note that reducing the supply pressure to the damper allowed air to be entrained resulting in a compressible fluid mixture and a drastic reduction in damping which lead to the larger vibration orbit. The loss of damping is not instantaneous, and in itself is not nonlinear, but eventually leads to an increase in amplitude and a jump up in vibrations. The increase in vibrations coupled with the reduction in damping may subsequently give rise to subharmonic and superharmonic vibration frequencies revealing nonlinear vibration behavior characteristics. The importance is shown in Figure 15 of supply pressure to the damper in eliminating the gaseous cavitation and nonlinearity resulting from the low damping present at these conditions. Note that when cavitation is suppressed by increasing the supply pressure to the damper as shown in the bottom cascade spectrum, both subharmonic and superharmonic vibrations are eliminated. The synchronous response is also much lower.

It is important to distinguish the nonlinear response exhibited above for squeeze film dampers with the response commonly associated with rotordynamic instability. In the case of the squeeze film dampers, the response is bounded and stable even though it is rich with subharmonic and superharmonic frequencies.

#### THEORETICAL MODELS AND LABORATORY MEASUREMENTS

The research program on squeeze film dampers in the Turbomachinery Laboratory at Texas A&M University has led to a number of innovations in damper technology, such as a patented feed and seal configuration which produces a more uniform pressure field around the damper. The experimental work has concentrated on the measurement of pressure fields and fluid film forces in damper test rigs with constrained journal motions of the circular type. The analytical work focuses on developing sound theoretical models and efficient computational tools for the prediction of SFD pressures and dynamic forced responses. State-of-the-art analyses address the effects of fluid inertia, fluid compressibility, end seals, and inlet feeding devices on damper

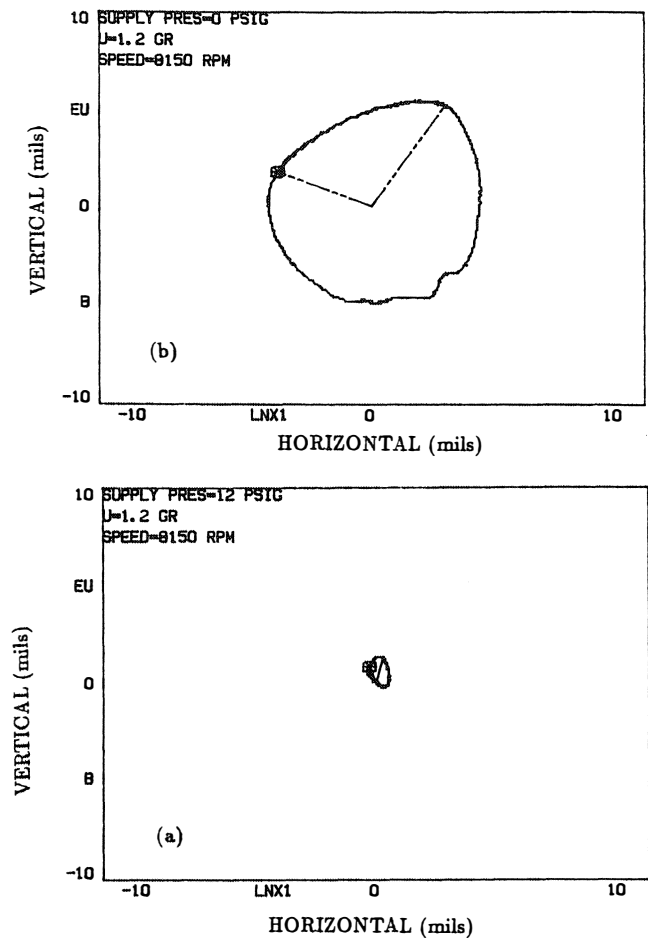


Figure 14. Rotor Orbits Showing the Influence of Cavitation on Vibration Amplitudes.

performance. Dynamic cavitation of thin fluid films and the actual coupled interaction between dampers and the rotor-bearing system are the most relevant and yet least understood issues.

Most dampers in practice are of short axial length ( $L/D < 0.25$ ) and accommodate some type of end seals to increase their damping capability. Additional features of this mechanical element may include high resistance orifices for pressure delivery and discharge, and deep grooves acting as flow sources or sinks of uniform pressure. Numerical analysis for the prediction of squeeze film pressures and computation of dynamic SFD forces are available in the open literature (Marmol and Vance [43], Szeri, et al. [44], and Kinsale and Tichy [29]).

Fluid film forces and force coefficients in SFDs are conveniently divided into two major types and related to the particular journal center motion. For unbalance response studies, SFD forces are obtained under the assumption of constant amplitude circular centered orbits; while for critical speeds calculation and stability analysis, SFD force coefficients are obtained for dynamic journal motion perturbations about a static equilibrium position.

#### SFD Rotordynamic Force Coefficients

Fluid film forces generated by small amplitude motions about an off-center equilibrium (static) position are of importance for stability analysis of rotating machinery employing SFDs. The SFD geometry and a journal performing closed motions of small



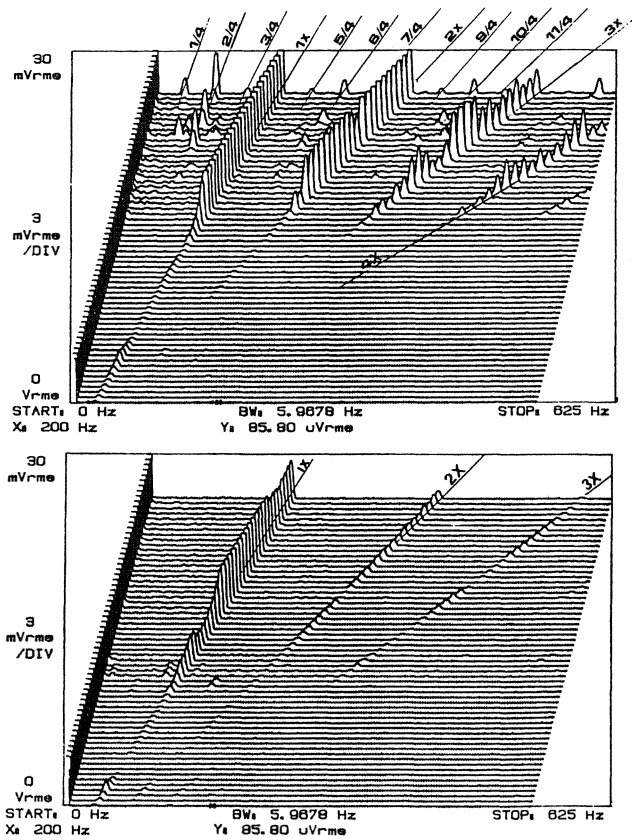


Figure 15. Influence of Supply Pressure on Suppressing Cavitation and Nonsynchronous Vibrations.

amplitude are shown in Figure 16 at an off-centered static position denoted by ( $e_s$ ). In general, the damper forces are given as:

$$-F_X = C_{XX} V_X + C_{XY} V_Y + M_{XX} A_X + M_{XY} A_Y \quad (1)$$

$$-F_Y = C_{YX} V_X + C_{YY} V_Y + M_{YX} A_X + M_{YY} A_Y$$

where ( $V_X, A_X$ ) and ( $V_Y, A_Y$ ) are the journal center instantaneous velocities and accelerations in the X and Y directions, respectively. And ( $C_{ij}, M_{ij}$ )<sub>ij = XY</sub> are the SFD damping and inertia force coefficients, respectively. Note that a squeeze film damper does not possess true stiffness coefficients since this mechanical element is not able to develop hydrodynamic pressures in the absence of journal motion. On the other hand, squeeze film dampers are sometimes referred to in the literature as having a dynamic stiffness [45]. One should notice that the so-called dynamic stiffness is always frequency dependent. That is, it disappears when the whirl velocity is zero. "Dynamic stiffness" is actually cross coupled damping ( $C_{ij}$  in (2) later) as explained in Vance [3]. Also, dampers with large levels of external pressurization may develop a hydrostatic stiffness as recent measurements show [30].

For short length open ends SFDs, the rotordynamic force coefficients are presented in APPENDIX as functions of the static eccentricity ( $\epsilon = e_s/C$ ). San Andres and Vance [24] also present the linearized force coefficients for finite length, open ends SFDs. The approximate formulae based on a correction to the long SFD model correlate well with a finite difference computational program. The interested reader may find this simple analysis readily accessible for his/her particular needs.

Robison, et al. [46], provide experimental verification of SFD rotordynamic coefficients using impact load excitations and a

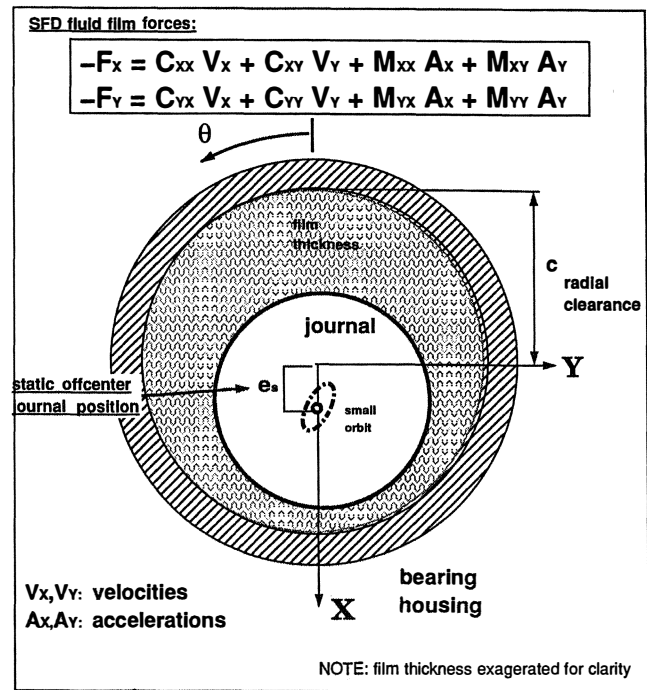


Figure 16. Schematic View of Journal Center Motion for Small Amplitude Displacements About an Off-Center (static) Position.

frequency domain technique to identify the force coefficients. The test damper article has a length, diameter and radial clearance equal to 46 mm, 127 mm and 0.133 mm, respectively. Tests were conducted at various off-center journal positions, three lubricant temperatures, and increasing levels of impacts resulting in journal motions with amplitudes to 30 percent of the damper clearance. The (dimensionless) direct damping and inertia coefficients,  $C_{XX}$  and  $M_{XX}$ , are shown in Figures 17 and 18 as a function of the static journal position ( $\epsilon$ ), which is also aligned with the direction of the imposed external load. The continuous lines in the figures correspond to the theoretical predictions based on a cavitated ( $\pi$ -film) model and show the coefficients to increase rapidly (nonlinearly) as the journal static position grows towards the bearing clearance. On the other hand, the experimentally identified force coefficients show little variation with the static position, and most importantly, appear not to be affected by the magnitude of the impact loads. In the experiments, no crosscoupled force coefficients were identified, indicating that the test SFD did not show the lubricant cavitation extent assumed by the theoretical predictions.

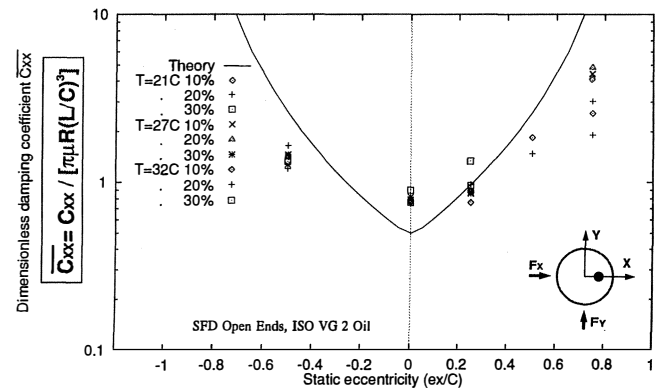


Figure 17. Dimensionless Experimental and Theoretical Direct Damping Coefficient  $C_{XX}$  Vs Static Eccentricity. Fluid film temperature and magnitude of impact vary.

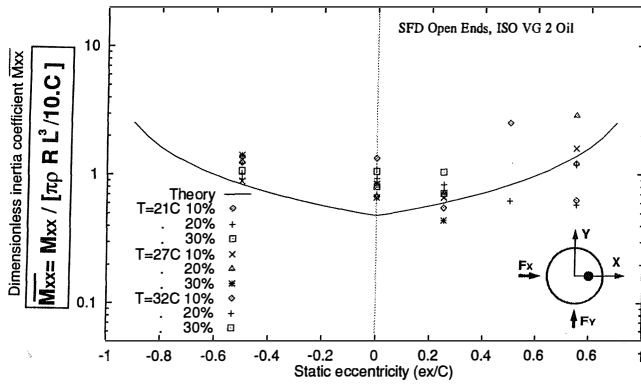


Figure 18. Dimensionless Experimental and Theoretical Direct Inertia Coefficient  $M_{xx}$  Vs Static Eccentricity. Fluid film temperature and magnitude of impact vary.

SFD Force Coefficients for Circular Centered Orbits

For circular centered journal motions of amplitude ( $e$ ) and whirl frequency ( $\omega$ ) in a perfectly cylindrical bearing, a damper produces a constant fluid film force in a reference frame rotating with angular frequency  $\omega$  (Figure 19). The radial and tangential components of the fluid film force are equal to:

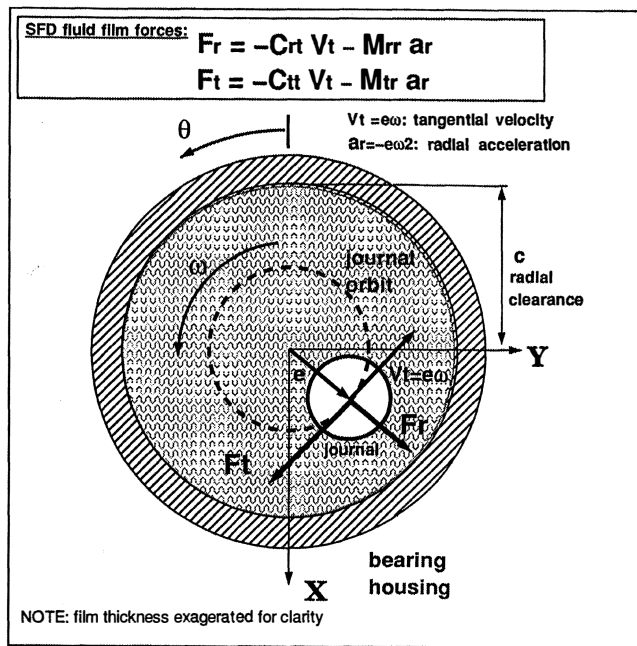


Figure 19. Schematic View of Journal Center Motion and Fluid Film Forces for Circular Centered Orbits.

$$F_r = -C_{rt} V_t - M_{rr} a_r, \quad F_t = -C_{tt} V_t - M_{tr} a_r \quad (2)$$

where  $V_t = e\omega$  and  $a_r = -e\omega^2$  are the tangential speed and normal acceleration of the whirling journal center, ( $C_{rt}$ ,  $C_{tt}$ ) and ( $M_{rr}$ ,  $M_{tr}$ ) are the cross and direct damping and inertia force coefficients, respectively. Note that these are not strictly rotordynamic coefficients as their classical definition implies small amplitude motions (perturbations) about a journal equilibrium position. For the short-length, open ends SFD model, the force coefficients using the rather simplistic  $\pi$ -film assumption (i.e., half the circumferential film extent is cavitated) are given as [3]:

$$C_{rt} = \frac{2\mu RL^3 \epsilon}{c^3(1-\epsilon^2)^2}; \quad C_{tt} = \frac{\pi\mu RL^3}{2c^3(1-\epsilon^2)^{3/2}}$$

$$D_{rr} = \frac{\pi\rho RL^3}{12c} \frac{[1-(1-\epsilon^2)^{-1/2}]}{\epsilon^2} \left(1-2[1-\epsilon^2]^{1/2}\right)$$

$$D_{tr} = -\frac{\rho RL^3}{c} \left(\frac{27}{70\epsilon}\right) \left[2 + \frac{1}{\epsilon} \ln\left(\frac{1-\epsilon}{1+\epsilon}\right)\right] \quad (3)$$

where ( $L$ ,  $D$ ,  $c$ ) denote the damper axial length, diameter, and radial clearance, respectively,  $\rho$  and  $\mu$  correspond to the lubricant density and viscosity, and  $\epsilon = e/c$  is the dimensionless orbit radius. For the full film model (no oil cavitation), the direct coefficients ( $M_{rr}$ ,  $C_{tt}$ ) are twice the value given above while there are no cross-coupled coefficients ( $M_{tr} = C_{rt} = 0$ ). The formulae given regard the lubricant as isoviscous and incompressible undergoing an isothermal process within a damper bearing and journal fully submerged in a lubricant bath. Large clearance, light viscosity SFDs operating at high frequencies are more affected by fluid inertia forces which introduce significant added masses and may change dramatically the dynamic response of a rotor SFD system [3]. Tichy, et al. [21], and San Andres and Vance [23] provide analysis for computation of fluid film forces in finite length dampers and including fluid inertia effects.

San Andres, et al. [28, 47], present measurements of dynamic pressures in a SFD rig with centered circular orbits to 50 percent of the damper clearance. Fluid film forces and force coefficients are extracted from integration of the measured pressure fields. The test damper, open on one end and sealed with an O-ring on the other end, has a length ( $L$ ) and diameter ( $D$ ) equal to 31 mm and 129 mm, respectively. Tests have been conducted with a large radial clearance ( $C$ ) equal to 1.6 mm to demonstrate the effect of fluid inertia [28], and with a reduced clearance equal to 0.381 mm more in accordance with actual industrial configurations [47]. The measured direct ( $C_{tt}$ ) and crosscoupled ( $C_{rt}$ ) damping coefficients are depicted in Figures 20 and 21 for a range of lubricant viscosities and for increasing whirl frequencies from 1,000 to 5,000 cpm. The test direct damping coefficients,  $C_{tt}$ , lie within the theoretical predictions for the full film and  $\pi$ -film models, i.e., at low whirl frequencies the measurements agree well with the uncavitated 2- $\pi$  model while at high frequencies, the measured values correlate well with the  $\pi$ -film model. The cross damping coefficients,  $C_{rt}$ , are smaller than the theoretical values for low lubricant viscosities where the extent of the cavitation zone is certainly less than the  $\pi$ -film assumption.

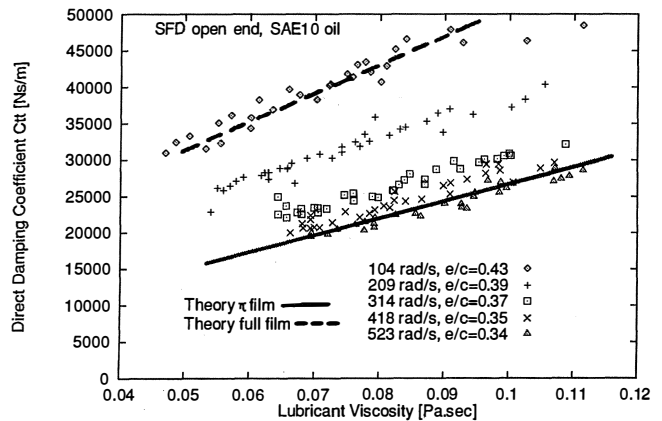


Figure 20. Open End SFD Direct Damping Coefficient  $C_{tt}$  Vs Lubricant Viscosity Measurements and Predictions from Short Length  $\pi$  Film Model.

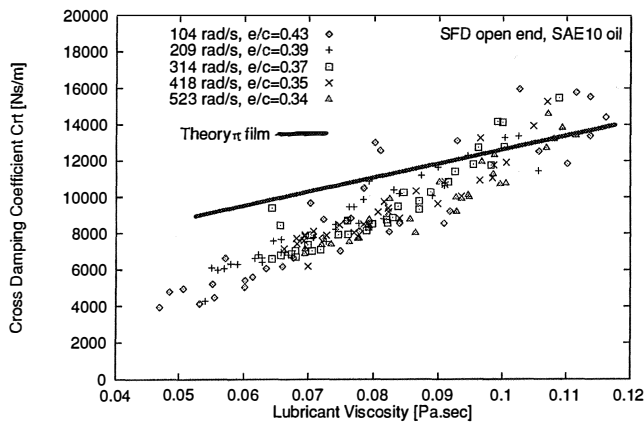


Figure 21. Open End SFD Cross Damping Coefficient Vs Lubricant Viscosity Measurements and Predictions from Short Length  $\pi$  Film Model.

The correlation of measured damper forces with predictions based on hydrodynamic lubrication theory ranges generally from poor to adequate. SFD forced performance is affected by a number of parameters and phenomena not included in the analytical models and simplified formulae given above. The level of lubricant inlet pressurization, the inlet feeding, and end sealing conditions are the most relevant for practical applications. The design and implementation of a SFD for rotating machinery can not rely solely on the indiscriminate application of some simple and highly idealized formulae, but rather on the knowledge of the machine operational characteristics and environment and the desired performance improvement.

## DESIGN PROCEDURE FOR SQUEEZE FILM DAMPERS

Most squeeze film dampers used in the field have been designed by copying past experience, with some amount of intuition thrown in for good measure. This has not always been an intelligent approach, especially when the design was not at least "ball park" confirmed by the design analysis tools which have been developed. For example, aircraft engine designers around 1970 had a strong predilection to specify the radial clearance as 3.0 mil, regardless of the rotor size, speed, and mass, because 3.0 mil was the most successful clearance used by Cooper [2] in his experiments at Rolls Royce. Some designers also believed that the squeeze film clearance would subtract from the available tip clearance around compressor blades. Experiments and analysis have since shown that the radial squeeze film clearance must be at least 2.3 times the local imbalance in order for the damper to be effective, and that the clearance is a strong factor in determining the damping coefficient, which has an optimum value for each different application. Also, the SFD often makes more clearance available for compressor blade tips, especially at critical speeds. It is true, however, that most SFD designs are severely constrained in their size and shape by the available space around the bearing, so most designs will continue to be strongly influenced by past experience with similar machines.

For those who want to use existing engineering knowledge to influence their design, the authors suggest the following general procedure and guidelines:

- Consider which rotordynamic phenomena the SFD will be designed to suppress, i.e., response to imbalance at the critical speeds, or subsynchronous instability. Conduct rotordynamic computer simulations to determine the optimum damping

coefficients required to suppress the selected phenomena. At this point, it will sometimes be discovered that no amount of damping at the bearings has a significant effect on the selected phenomena because the bearings are located near the nodes of the relevant mode shapes. For aircraft engine applications, such a discovery makes the remaining procedure irrelevant unless the mode shapes can be changed by rotor modifications or by softening the squirrel cages. For industrial compressor applications the squeeze film and O-ring (or centering spring) flexibility will be in series with the tilt pad bearing, so both the resultant stiffness and damping will be less than the coefficients of the tilt pad bearing alone. The lowered resultant stiffness can move the nodes away from the bearing and make the available damping effective. The computer simulations should, therefore, be directed toward determining the required reduced stiffness value.

- Decide which geometry, lubricant feed mechanism, and end seals best fit the available space and configuration of the machine. Keep in mind that an annular feed groove provides the option of making it wider at a later date if the damping (or the effective SFD stiffness) turns out to be too large. This is especially important in industrial compressor applications where the damper is in series with the oil film bearing. Also keep in mind that piston ring end seals usually leak more than you expect. (O-ring seals generally have low leakage.) If the oil flow path does not directly go from the SFD to the bearing, or if end seals are not used, take extra measures to provide ample scavenging to return the leakage to the sump.

- After the SFD geometry, feed mechanism, and end seal type have been chosen, obtain access to equations or computer codes which are applicable to the configuration and use them to calculate the force coefficients of the squeeze film at the whirl frequencies of interest. The calculated coefficients will probably have a large error unless your damper has: a) no end seals, b) narrow lands (short bearing), and c) high supply pressure of the same order of magnitude as the peak pressure in the squeeze film. The coefficients for this case can be calculated fairly accurately from the full film version of Equation (3) above. It is often convenient to express  $D_{tr}$  as an added mass as explained in Vance [3]. If conditions a) and b) are satisfied, but not equation c), then the  $\pi$ -film version of  $C_{tt}$  in Equation (3) can be used and  $D_{tr}$  can be assumed to cancel out  $C_{tt}$  at high Reynolds numbers. For an aircraft engine application, these are the coefficients to use (after adding the squirrel cage stiffness) in the rotordynamic computer simulation to predict critical speed response or stability. For circular centered orbits,  $C_{tt} = C_{xx} = C_{yy}$ .

- For industrial compressor applications, the squeeze film coefficients calculated in the preceding step must be properly combined with the O-ring stiffness (they are in parallel so they add) and then these coefficients must be properly combined with the tilt pad oil film coefficients (they are in series). Nicholas, et al. [48], gives useful formulas for combining coefficients which are in series. Leader, et al. [45], shows how to measure the O-ring stiffness and how to use the Nicholas formulas. The most important factor for success in these cases is that the O-ring stiffness should not be too high. The resultant damping will always be less than the damping which is already in the tilt pad bearing, so the resultant stiffness must be reduced to allow the available damping to work. The third author measured the O-ring stiffness in one application with a heavy rotor and found it to be about 10 times the value reported by Leader, et al. [45]. Also, it should be realized that elastomeric materials have a dynamic stiffness that varies with frequency. The frequency dependence information can usually be obtained from the material supplier. Very high O-ring stiffness renders the squeeze film damper practically useless. In such cases, the O-ring should be supplemented by additional centering devices which retain relatively low stiffness characteristics under heavy loads.

Once the final resultant force coefficients are obtained, they can be input to the rotordynamic computer simulation to predict response or stability.

## APPLICATION OF SQUEEZE FILM DAMPERS

Squeeze film dampers have traditionally been used to overcome stability and vibration problems that are not adequately handled with conventional style bearings. One of the key design features in a squeeze film damper configuration is the introduction of support flexibility and damping in the bearing/support structure. This translates to lower transmitted forces and longer bearing life, particularly for machinery that are designed to operate at supercritical speeds. Machinery that run above the first critical speed are classified as supercritical and constitute an increasing number of the new high performance machinery manufactured today. The advantages of running supercritical becomes apparent when computing the forces transmitted to the bearings. Lower stiffness in the bearing supports will generally result in lower transmitted forces when operating supercritical. Lower damping (not more damping), as shown in Figure 22, will also result in lower transmitted forces. However, since some damping is required to allow for safe traversing of the critical speed, an optimum value must therefore be determined to satisfy the two rather conflicting requirements. This is why an optimization process is generally required to determine the "right" amount of damping.

This section describes some of the commonly used squeeze film dampers and introduces one of the more novel damper designs. Examples of the optimization process required in the design and selection of squeeze film dampers and their applications to solve stability and critical speed problems are also demonstrated.

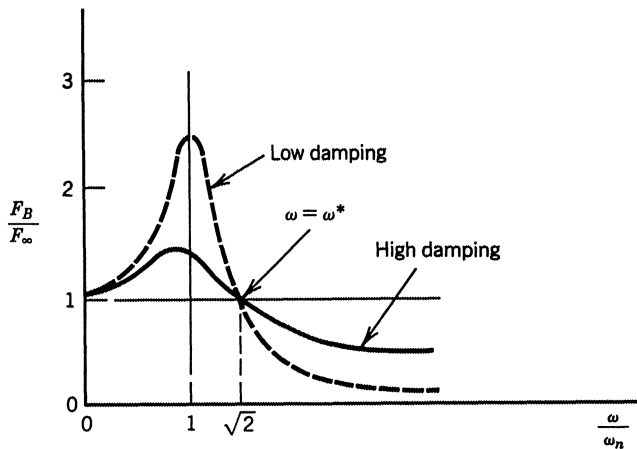


Figure 22. Influence of Damping on the Transmitted Force.

### Common Configurations and Applications

#### Squeeze Film Dampers without a Centering Spring

This is the simplest of the squeeze film damper configurations. The outer race of a rolling element bearing, or the bearing shell or retainer in the case of a fluid film bearing, is allowed to float and whirl in a clearance space between the bearing outer diameter and the housing inner diameter. The outer race or bearing shell forms the damper journal that is allowed to whirl, but is prevented from spinning or rotating by a "loose" antirotation mechanism. This "loose" antirotation configuration is necessary to allow the damper journal or outer race to whirl or orbit (not spin) in a precession motion, squeezing the oil in the small clearance space and generating an oil film pressure and, subsequently, a damping force.

The absence of a mechanical centering spring in this design configuration means that the damper journal will be bottomed out at startup. As the speed increases and the shaft starts to whirl, the damper's journal (bearing shell outer surface) will lift off. The oil film in a squeeze film damper does not produce stiffness (i.e., support a static load) like conventional fluid film bearings. However, the damper does develop stiffness-like behavior. This stiffness is due to the crosscoupled damping coefficients which exhibit frequency dependent stiffness-like (spring) characteristics.

The noncentered damper is one of the most nonlinear of the squeeze film damper designs. There are two basic mechanisms that are responsible for this nonlinear behavior. The first of the two nonlinear mechanisms is attributed to the nonlinear characteristics produced by the crosscoupled damping coefficients. The crosscoupled damping term (stiffness-like term) in a noncentered damper is very highly nonlinear at journal eccentricities above 0.7. The second source of nonlinear behavior present with this type of damper comes as a direct consequence of the bottoming out of the damper journal. This generally occurs at high side loads, or due to excessive unbalance forces. The bottoming out of the damper journal, which is very likely with this design due to the absence of a centering spring, will result in a bilinear spring behavior. This characteristic is illustrated by the stiffness vs amplitude plot shown in Figure 10. This nonlinear behavior can be inferred from the sub-synchronous and supersynchronous vibration characteristics often noted on this type of damper as shown in Figures 11, 12, and 13. In some cases, the impact force generated when the damper journal bottoms out excites the lowest natural frequency of the rotor, as was shown in Figure 12. In the case of flexible casings and support structures, the resonance frequencies of the structure can also be excited.

The noncentered dampers are commonly used on aircraft engine gas turbines, lightweight process compressor rotors, and automotive turbochargers. In aircraft engines, their use has been limited to the smaller engines where the use of a conventional style centering spring (squirrel cage spring) is difficult to implement due to space limitations.

#### O-Ring Supported Dampers

The simplest means of providing a centering spring in a squeeze film damper is through the use of elastomer O-rings. An illustration of this damper design is shown in Figure 23. The advantages of this design stem from its simplicity, ease of manufacturing, and the ability to incorporate the damper into small envelopes. The relatively low radial space required makes it the preferred method to retrofit existing machines in the field. The O-ring doubles as a good end seal, which helps increase the effectiveness of the damper by reducing side leakage. Some of the disadvantages with this design are attributed to the limited range of stiffness that can be achieved with elastomers. Predicting the stiffness with a good degree of certainty is difficult in elastomeric materials due to the material variance and the influence of temperature, frequency, and time on its properties. The elastomer stiffness and damping is strongly influenced by temperature. The O-ring design is also susceptible to creep, causing the damper to bottom out, which, as discussed above, may lead to a bilinear spring behavior.

O-ring dampers are not capable of taking thrust loads and cannot be easily manipulated for centering of the damper journal within the damper clearance space. One means of achieving some centering capability is through making the O-ring groove eccentric. This limitation makes them only suitable for use with lightweight rotors.

High speed and high pressure centrifugal compressors prone to stability problems frequently have been fitted with these O-ring dampers. The damper is installed in series with tilting pad fluid film bearings to enhance the stability of the compressor. Although

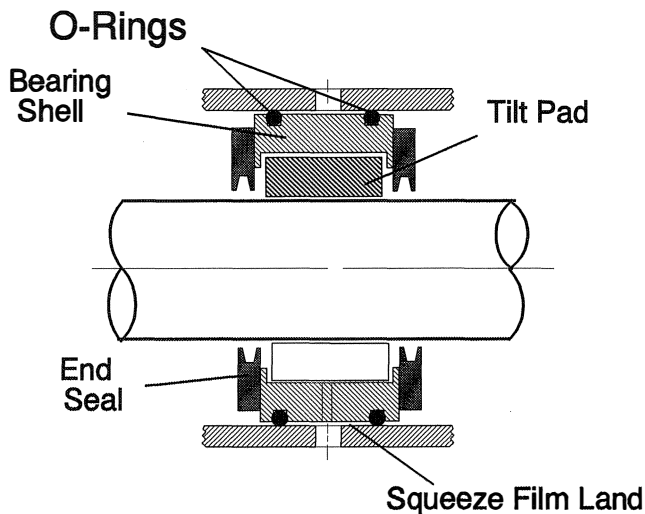


Figure 23. Schematic of an O-Ring Supported Damper.

most of their use has primarily been aimed at improving stability, they have also been used to reduce the synchronous response due to imbalance, or to shift the peak unbalance response outside the operating speed range.

The O-rings also provide a form of internal friction damping (hysteretic damping) in addition to the squeeze film damping (viscous damping) produced by the oil in the damper. The elastomer material of the O-ring limits the use of such dampers to mostly low temperature applications. The hysteretic damping from the O-rings has also been utilized in series with rolling element bearings, and gas bearings without any oil in the clearance space (dry O-ring damper). High speed dentist drills (hand pieces) are an example where this configuration has been implemented. These drills are composed of air turbines running on ball or gas bearings with elastomer O-ring supports for increased damping and improved stability.

#### Squirrel Cage Supported Dampers

This is the most commonly used squeeze film damper design, particularly in aircraft engines where its use is widespread. Most large aircraft gas turbine engines employ at least one, and in many instances, two or three of these dampers in one engine. A schematic of this damper is shown in Figure 24. A distinctive feature necessary with such a design (and apparent from the schematic), is the relatively large axial space required in comparison to the damper length. This is one of the major drawbacks of this damper design. The squirrel cage forming the centering spring for the damper quite often requires three to four times as much axial space as the damper itself.

Assembling the squirrel cage spring and centering the journal within the clearance space requires special tools and skills. The squirrel cage spring also complicates the damper end seal design and assembly. It is also very difficult to offset the spring assembly in order to account for the gravity load due to the shaft weight. Maintaining parallelism between the damper journal and housing is another factor that adds uncertainty and complications to this design.

The squirrel cage damper is not as highly nonlinear as the previous two configurations described, and the stiffness characteristics are easily modelled and can be predicted with a high degree of certainty. However, they still exhibit nonlinear characteristics due to cavitation in the oil film. Nonlinear characteristics can also be present due to the bilinear spring effect apparent when the damper is not properly centered and during operating conditions that lead to the damper bottoming out.

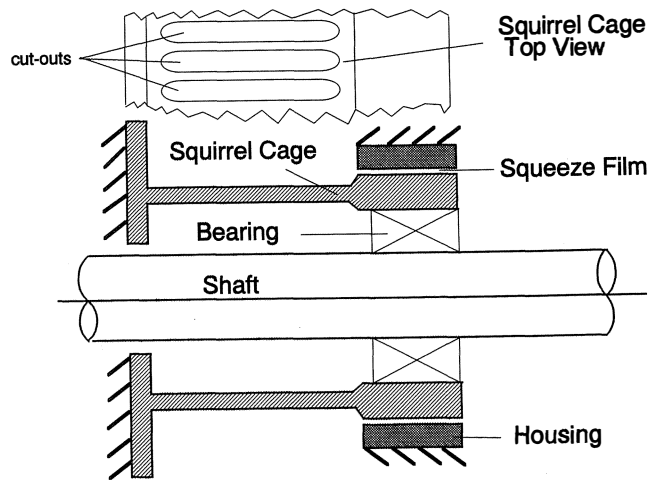


Figure 24. Schematic of a Squirrel Cage Supported Damper.

#### Integral Centering Spring Damper

An integral centering spring squeeze film damper is shown in Figure 25. The cantilevered support ribs, along with the sector they are supporting at both ends, form a centering spring element. The small gap between the sector and the outer ring forms the squeeze film damper clearance space. The complete assembly can contain any number of sectors depending on the load and required stiffness and damping for the particular application. The sectors in the lower half of the damper carrying the rotor weight can also be machined with an offset to counter the deflections caused by the rotor weight. More than one stiffness range can be achieved by using an additional pivot located at a specified distance from the support rib. This can provide a more gradual nonlinearity that is desirable in cases of excessive unbalance or side force. Such a configuration will help in absorbing impact loads, high side loads, and high vibration excursions due to traversing the critical speeds or a blade loss. The circumferential location of the stop pivot and the gap between the pivot end and the support rib are two additional design variables that provide additional flexibility.

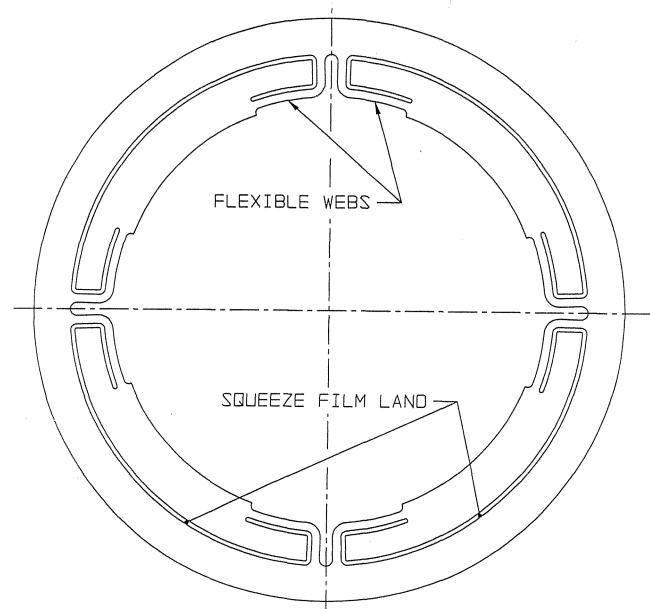


Figure 25. Schematic of an Integral Centering Spring Damper.

This novel centering spring squeeze film damper design does not occupy any additional axial space beyond the existing length occupied by the bearing. This is a major advantage over conventional squirrel cage type damper supports which in contrast require three to four times the axial space occupied by the damper or bearing. Furthermore, unlike the first two damper configurations (noncentered and O-ring supported dampers), the new design is capable of absorbing axial thrust loads without locking the damper's radial motion.

The integral design makes manufacturing, assembly, and inspection much easier and more reliable than any other configuration. The squeeze film gap can be made with very good precision utilizing this concept. Wire electric discharge machines (EDM) provide an excellent means of obtaining the desired clearance with very high precision and repeatability maintaining excellent parallelism between the damper journal and housing. Damper retrofit in process type equipment, which are required to meet API specifications dictating a split bearing configuration, can be easily accommodated with this new concept. This design unlike conventional style dampers, can be easily provided in a split configuration as shown in Figure 26.

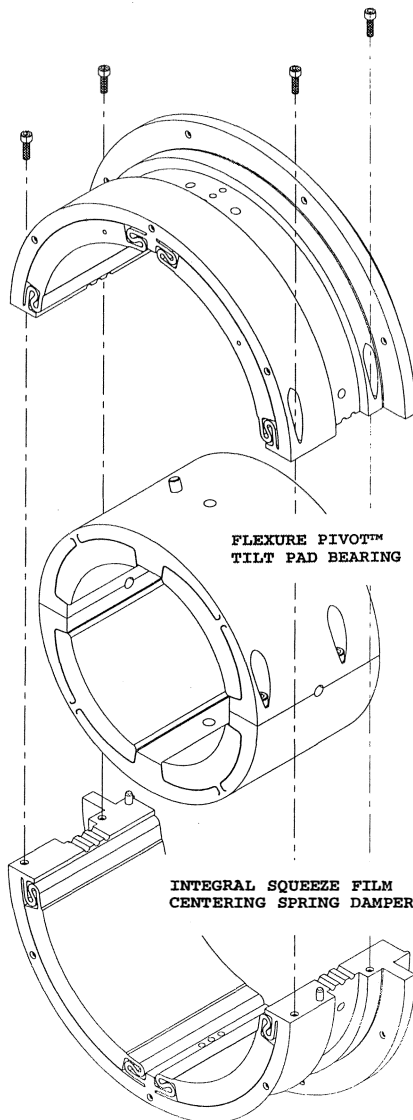


Figure 26. Three Dimensional Schematic of a Split Integral Centering Spring Damper.

#### Example Cases of Squeeze Film Dampers Optimization for a Process Compressor

In process equipment, squeeze film dampers are used primarily to improve rotordynamic stability. They are usually used as a last resort due to the complexity and drawbacks inherent in conventional dampers. The difficulty associated in accurately predicting damper performance due to lubricant cavitation, is another reason for their limited use. The new damper design with the integral centering spring overcomes many of these difficulties as shown by the following example.

This example demonstrates the importance of the centered damper in suppressing the subsynchronous vibration exhibited by the relatively heavy rotor shown in Figure 27. This rotor was supported by O-ring type dampers but continued to exhibit subsynchronous vibrations after the damper retrofit. Rotordynamic stability without the squeeze film damper is very low as indicated by the low logarithmic decrement predicted for the first forward mode shown in Figure 28. The rotor is much more flexible than the bearings, resulting in very small motion at the bearing supports and consequently low effective damping. The bearings are virtually at a node and, therefore, are ineffective in suppressing the subsynchronous vibrations.

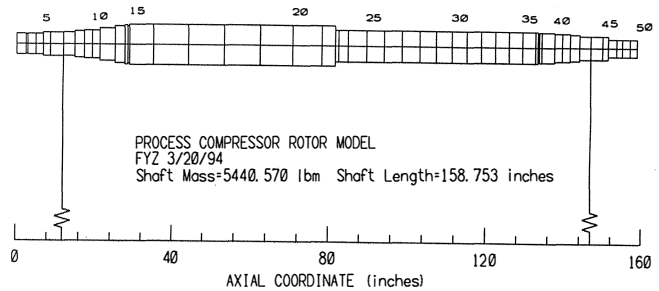


Figure 27. Process Compressor Rotordynamic Model.

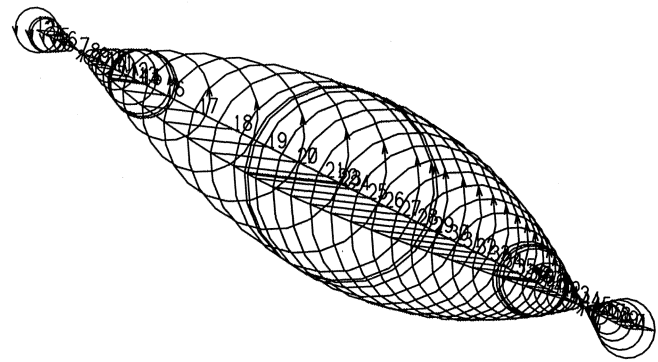


Figure 28. First Forward Mode without the Squeeze Film Damper.

The use of a squeeze film damper in series with the tilting pad bearings will introduce flexibility and damping to the bearing support. The damping provided by the squeeze film damper however, must be optimized, as shown in Figure 29. Low values of damping may not be sufficient and high damping may lock the damper and reduce the effective damping as evident by the reduction in the logarithmic decrement at high values of damping.

Using the optimum damping value and varying the squeeze film support stiffness showed that a more flexible spring support will allow motion at the bearing, resulting in more effective damping, and thus suppression of the instability and subsynchronous vibrations. However if the damper bottoms out, as was the case with the

**SQUEEZE FILM DAMPER OPTIMIZATION**  
 LOGARITHMIC DECREMENT AS A FUNCTION OF DAMPING

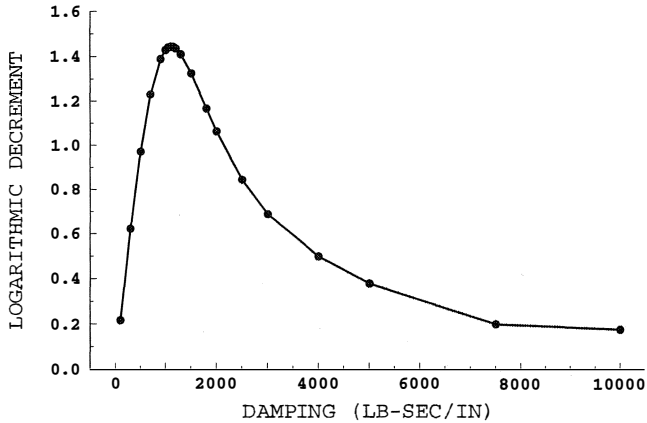


Figure 29. Squeeze Film Damping Coefficient Optimization.

O-ring damper, the stiffness will increase and the damper becomes ineffective as evident by the high support stiffness values on the right portion of the logarithmic decrement curve shown in Figure 30. The damper is very effective when the damper journal (tilt pad bearing shell OD) can be held close to the centered position within the damper clearance space. This is very difficult to accomplish with the conventional O-ring dampers, particularly in the case of relatively heavy rotors.

**DAMPER SPRING STIFFNESS OPTIMIZATION**  
 DAMPER DAMPING FIXED AT 1100 LB-SEC/IN

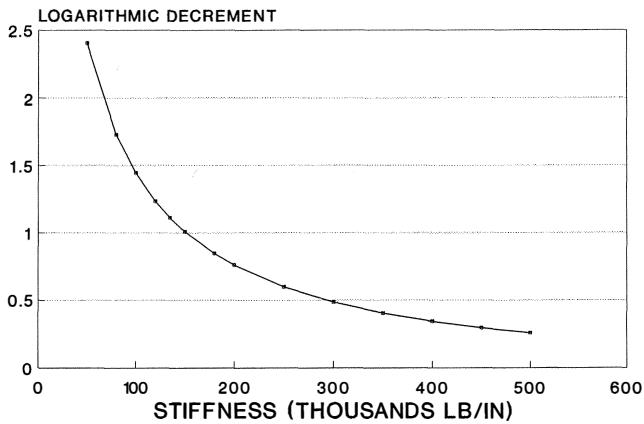


Figure 30. Squeeze Film Centering Spring Optimization.

The use of an integral centering spring damper configuration allows precise location of the damper journal and realization of the required stiffness value. In order to achieve the low stiffness values while still maintaining lower stresses, the damper configuration shown in Figure 31 was utilized. The "S" shaped flexible elements were required to keep the stiffness and stresses low due to the relatively heavy rotor weight. The wire EDM technology allows the production of such a damper device which can be easily designed with an offset to compensate for the deflection due to rotor weight.

The stability of the rotor-bearing system was greatly improved with the optimized squeeze film damper. This is evident by the relatively high logarithmic decrement for the first forward mode shown in Figure 32. The flexibility introduced with the integral centering spring allows for motion at the bearings, thus making the damping more effective.

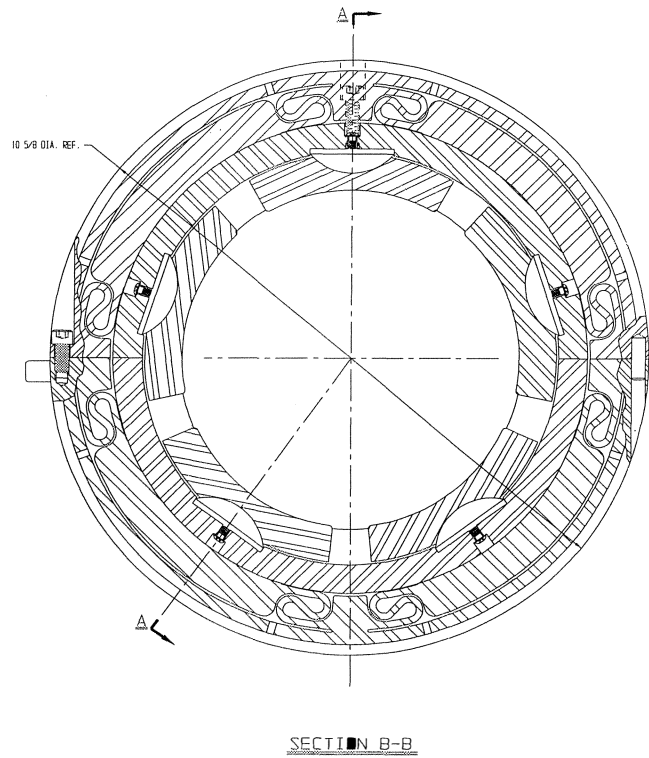


Figure 31. "S" Shaped Integral Centering Spring Damper.

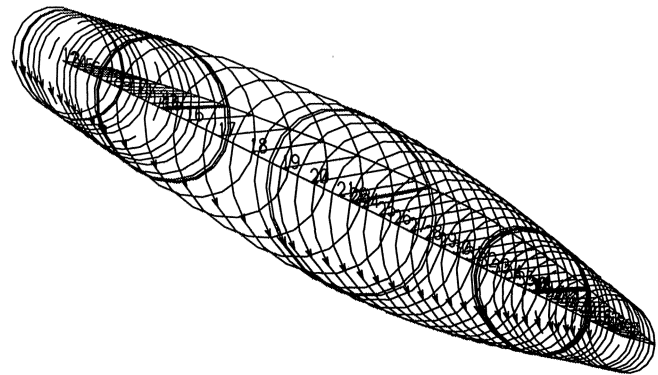


Figure 32. First Forward Mode with Optimized Squeeze Film Damper.

*Damper For Control Of Critical Speed*

The squeeze film damper in series with a fluid film bearing also provides a means for improving the synchronous response, an advantage rarely utilized with process type equipment. The tight vibration restrictions with the latest API specifications and the even more restrictive specifications dictated by the users, makes the squeeze film damper a very attractive and practical alternative to other costly and time consuming designs. The squeeze film damper will help in reducing the sensitivity to unbalance that often results in significant delays during shop testing and commissioning of process type equipment. The following example shows how the squeeze film damper softer support can shift the critical speed down, removing it from the operating speed range.

The undamped critical speed for a process steam turbine is shown in Figure 33. The turbine operating speed range was too close to the first critical speed which forced operation at higher

speed than necessary for process requirements consuming more steam in order to maintain acceptable vibration levels. A stiffer bearing as evident by the undamped critical speed map, will not help in this case. Higher bearing stiffness will have a minor effect on the critical speed, if any, and will shift the critical closer to the running speed, which is not the direction sought in this application. The oil film stiffness in the existing bearing cannot be made any softer since the sleeve bearing configuration in use is one of the softest fluid film bearings available. Therefore, a drastic reduction in the bearing supports can only be achieved by incorporating a squeeze film damper in series with the fluid film bearings. The response comparison shown in Figure 34 demonstrates the distinct advantages made possible with the squeeze film damper.

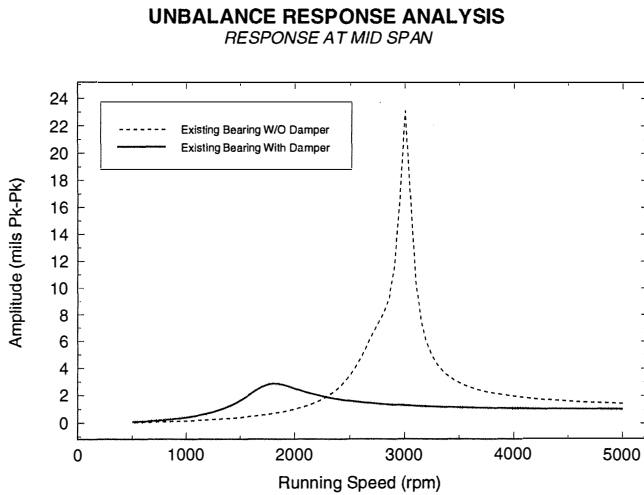


Figure 33. Bearing Support Coefficients with and without the Squeeze Film Damper Superimposed on the Undamped Critical Speed Map.

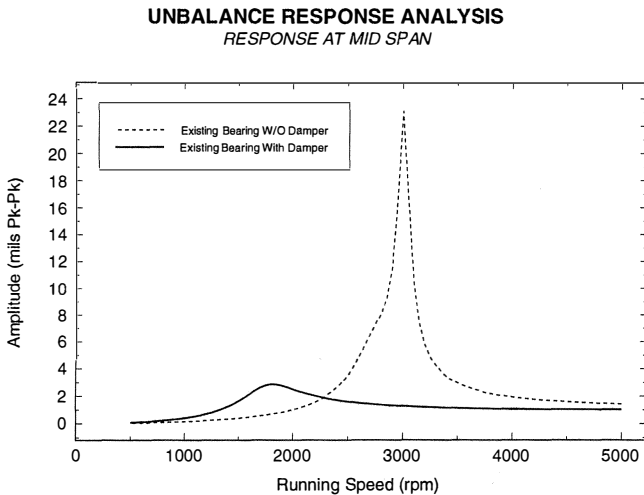


Figure 34. Synchronous Response with and without the Squeeze Film Damper.

*Damper Design for Control of Unbalance Forces*

One of the primary limitations in conventional style dampers is their inability to center a relatively heavy rotor. Murphy [49] shows a schematic of a high speed compulsator required to operate at speeds ranging from 8000 to 12,000 rpm with high radial and

thrust forces experienced during discharge. The integral centering spring damper supplied is shown in Figure 35 and was capable of providing 800 lb-sec/in of damping. The predicted response is shown in Figure 36 compared to the measured response during testing. This accuracy in predicting the stiffness and damping with this style of damper is another very desirable feature that has been missing with conventional damper designs.

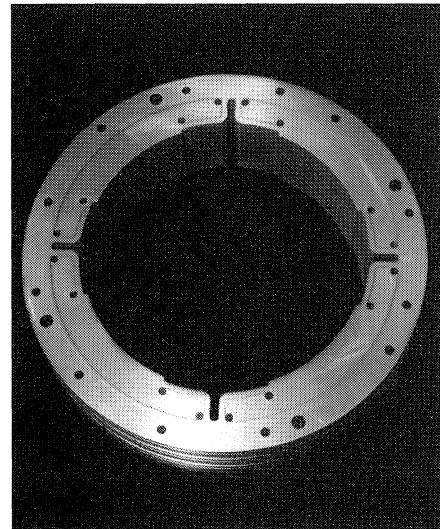


Figure 35. Integral Centering Spring Damper Used to Support High Speed Compulsator.

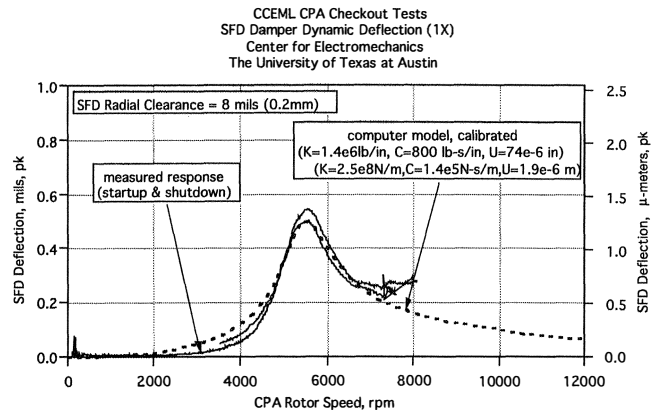


Figure 36. Comparison Between Measured and Predicted Response with Integral Centering Spring Damper.

*Damper Design For a Turboprop Engine Rotor*

A company in Texas is considering the development of a new turboprop engine for general aviation. Some exploratory designs of the gas generator and power turbine rotor-bearing systems have been tested full scale and full speed by the third author and his research assistants in the Turbomachinery Laboratory. The tests were designed to confirm computer predictions of critical speeds and to evaluate the performance of the squeeze film dampers over the expected range of oil supply temperatures and pressures. The computer predictions are from XLROTOR, a transfer matrix code developed by Murphy [50].

Each rotor tested to date has had two bearings and each bearing has a squeeze film damper. The damper and squirrel cage were first designed for the gas generator rotor, and it was decided to use the same hardware for the power turbine rotor, which is smaller and



lighter. The damper and squirrel cage design is constrained by the available space, but a clever feed groove and seal design was provided by the engine designer, which appears to greatly reduce the propensity for air injection into the oil. End seals are used in an effort to induce most of the oil to flow from the squeeze film land to the roller or ball thrust bearing. Early tests of the gas generator rotor provided the incentive for some redesign of that rotor, and the power turbine rotorbearing system was tested in the interim. The redesigned gas generator rotor is being tested at the time of this writing. The results reported here are for the power turbine. A cross section is shown in Figure 37 of the power turbine test rotor mounted on the squirrel cages which in turn are installed in support pedestals in the test cell. Figure 38 shows one of the squirrel cage and squeeze film damper assemblies.

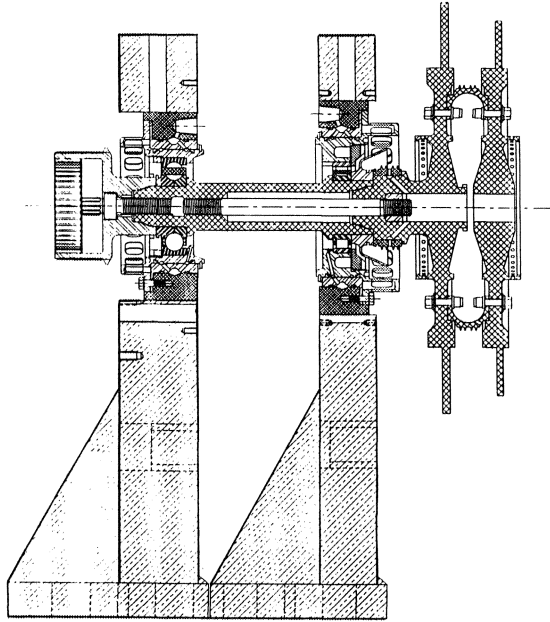


Figure 37. Power Turbine Rotor on Squirrel Cage Supports with Squeeze Films.

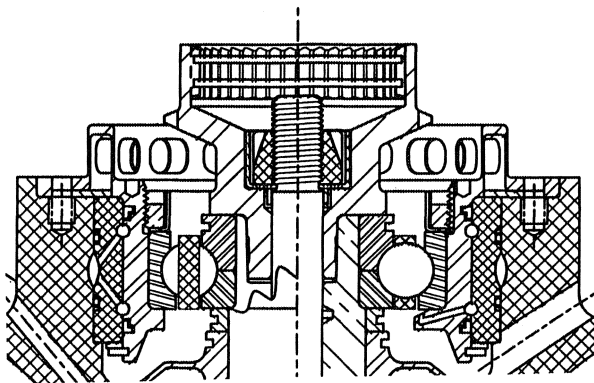


Figure 38. Squirrel Cage with a Squeeze Film Supporting a Ball Bearing.

One of the most difficult tasks in the test program was measurement of the squirrel cage stiffness. This value must be low enough to place the first two critical speeds below idle. Low stiffness also allows the squeeze film to operate effectively. An accurate value is essential so that the stiffness that produces measured critical speeds will not be incorrectly ascribed to the squeeze film. Calculations were performed using elastic deflection formulas

(each rib of the squirrel cage is modelled as a beam with built in ends). After the rotor was installed on the squirrel cages, a crane and hoist was used to apply measured forces to the rotor at a position adjacent to the squirrel cage. Rotor deflection was measured with a dial gauge indicator. The resulting stiffness values did not agree with the calculations, so the rotor was removed and a test fixture was designed for the squirrel cage alone. Stiffness measurements on the test fixture did agree well with the calculations. In the first tests with the rotor in place, the rotor had been bending, so the deflection was not the squirrel cage alone. The rotor was reinstalled on the squirrel cages and nonrotating free vibration rap tests produced natural frequencies that agreed well with computer simulations using XLROTOR.

Squeeze film force coefficients were computed using COEFCCO, a code developed by the second author for SFD with end seals. One of the inputs to the code is a number  $C_L$ , which represents the end seal leakage. This value must be estimated from our experience with SFD test rigs having different kinds of seals. Looking at the hardware, it appeared that the design would have low leakage, so a relatively low value of 1.0 was assigned to  $C_L$ . Later tests would show that this value (the leakage coefficient) was greatly underestimated at low temperatures but overestimated at high temperatures. This can be explained by considering the thermal expansion of the metal end seal rings. It is not realistic to assume that one can guess the leakage coefficients correctly without test data for the exact same configuration under the expected operating conditions.

The test plan called for oil supply temperatures to vary from 80°F to 250°F, so damper force coefficients were computed over this range of temperatures. The effective direct damping coefficients (including fluid inertia contributions) predicted by the code ranged from a high of 251 lb-s/in at the lowest temperature down to only 12 lb-s/in at the highest temperature.

Imbalance response can be predicted accurately by computer models only if the imbalance is a known quantity. Magnitude, phase, and location in the rotor of the imbalance are all required inputs to rotordynamic computer codes. In this case, the simple geometry of the overhung rotor with the turbine wheels close together dictates that most of the imbalance is at the wheels. Trim balance measurements on the test rig with trial weights established the magnitude and phase which were used in the computer simulation. The response to imbalance is shown in Figure 39 measured on the test rig with 94°F lubricant temperature at the inlet to the squeeze film. The plotted amplitude is filtered at the synchronous frequency with the runout subtracted using ADRE, a signal analysis system. The response predicted by XLROTOR is shown in Figure 40 with the predicted damping coefficients from COEFCCO at 95°F using a leakage coefficient  $C_L = 5.0$ .

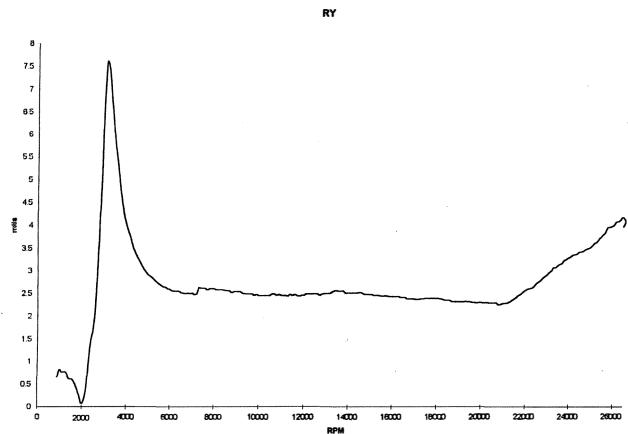


Figure 39. Measured Response to Imbalance at 94°F Oil Temperature.

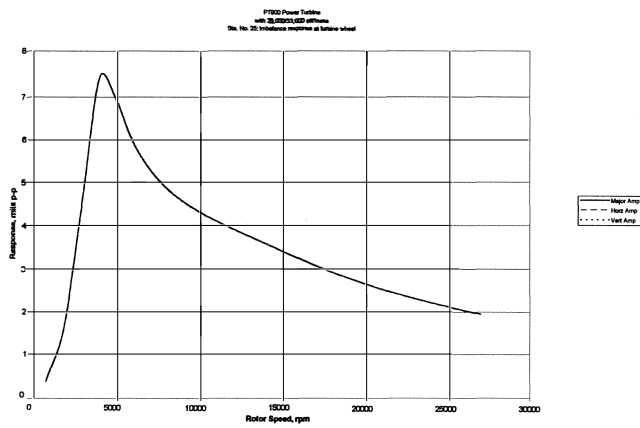


Figure 40. Computer Simulation of the Response Shown in Figure 15.

The synchronous response measured on the test rig at 210°F temperature is shown in Figure 41. The response predicted by XLROTOR is shown in Figure 42 with damping from COEFCCO at the same temperature but with the leakage coefficient changed to  $C_L = 0.6$ .

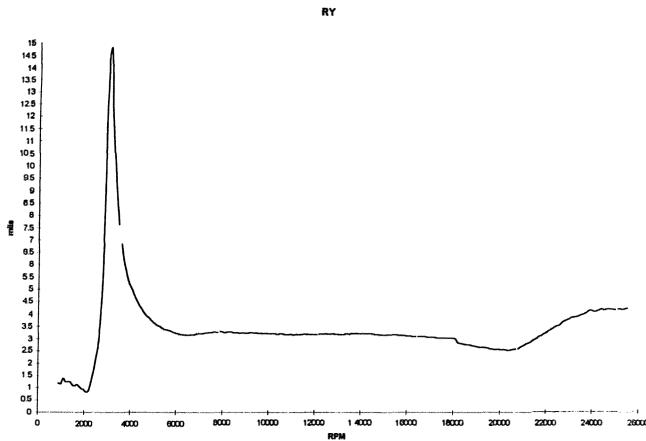


Figure 41. Measured Response to Imbalance at 210°F Oil Temperature.

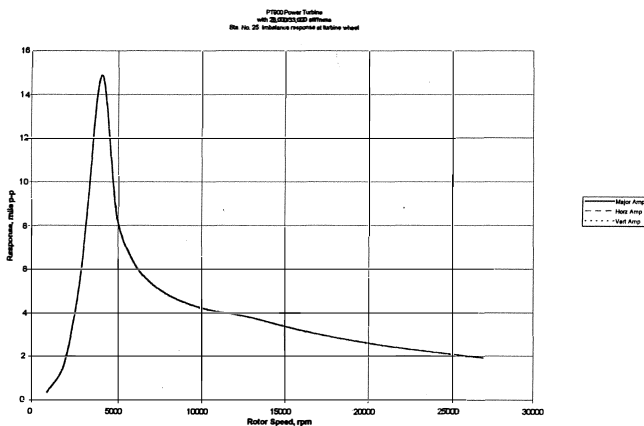


Figure 42. Computer Simulation of the Response Shown in Figure 17.

Comparisons of the measured and computed plots show remarkable agreement, but the leakage coefficient had to be adjusted to

the smaller value at the higher temperature in order to obtain this agreement. The simulation is excellent, but only after using the test data to determine the correct leakage coefficient for the end seals at the two temperatures. All of the responses shown here were computed and measured at the outboard turbine wheel. The response at the coupling end is slightly more complex but the computer simulation is excellent there as well. Notice on Figure 39 that the response is increasing at maximum speed, whereas on Figure 41 (at higher temperature with less damping) the rate of increase is much less. In Figure 39, the damping forces are bending the rotor shaft. This illustrates the requirement for optimum damping.

Air ingestion was not directly included in the squeeze film analysis for this example although an air/oil mixture is routinely observed in the return lines from the dampers on this test rig. Cavitation was represented by the simple  $\pi$ -film model as described in an earlier section. Thus, the effects of air ingestion and variable cavitation are included indirectly in the leakage coefficient required to obtain good agreement with the test results.

## CLOSURE

Squeeze film dampers are an excellent design tool that can be used to advantage in providing smooth running and reliable supercritical machinery. Its use in problem process machinery has tainted it as a "bandage" solution, and many users shy away from its use for this same reason. Another reason for their limited use is the difficulty in accurately predicting the performance, particularly with O-ring supported dampers.

Applications using squeeze film dampers in series with process fluid and water lubricated bearings can also be an area of high potential usage. The damper in this case provides much of the damping lost due to the use of low viscosity lubricants. The lower viscosity available with process fluid and water lubricated bearings has always been a major obstacle to their use. In those applications, the models developed by the second author could prove very valuable for modelling the fluid inertia effects which will dominate the performance of such dampers.

The advantages of squeeze film dampers highlighted in this article are numerous. However, care must be exercised in the proper design, selection, and manufacturing of these dampers. Determining the optimum value of damping is necessary to ensure the supports are not under or over-damped. Over-damped supports may lockup and significantly reduce the effective damping. The stiffness must be properly selected, and its influence on the location of the critical speeds and the bearing transmitted forces must be carefully accounted for in the analysis. Properly designed dampers will significantly increase the reliability and improve the vibration characteristics of new and existing rotating machinery. In series with rolling element bearings, SFDs can significantly increase bearing life and reduce vibrations and noise. The stability with existing fluid film bearings can therefore be extended. This should allow operation at higher speeds and possibly with longer spans between bearings. The balance limitations and threshold speeds on many of the existing machinery can then be extended.

If really accurate predictions of squeeze film force coefficients are to be made for all but the simplest configurations, extensive advanced research is required to investigate the detailed effects of fluid dynamic cavitation, two phase fluid flow, and end seals on damper performance. Realistically, it may not be practical, or even possible, to achieve the capability for accurate simulations of two phase flow within the foreseeable future.

Given the present lack of capability to predict two phase flows and pressures, and end seals leakage, it must be stated that the only reliable way to accurately know squeeze film force coefficients, for a particular squeeze film geometry with particular inlet conditions and particular end seals, is to perform full speed tests on full scale

SFD hardware with operational supply pressures, oil temperatures, and surrounding gas atmospheres. However, many users have not done this, and since the preponderance of applications have been successful, it can be seen that the SFD is generally a forgiving device and the chances of success are fairly good if the design procedures and warnings suggested in the tutorial are followed. The low stiffness of most squeeze film dampers is probably more responsible for their success than the damping, especially in industrial compressor applications.

APPENDIX

Linear Force Coefficients for Open Ends SFDs		
	Full film solution (no cavitation)	$\pi$ -film cavitated model
$C_{XX}$	$\mu D(L/C)^3 \frac{\pi(1+2\epsilon^2)}{2(1-\epsilon^2)^{2.5}}$	$\mu D(L/C)^3 \frac{[3\epsilon+i(1+2\epsilon^2)/2]}{2(1-\epsilon^2)^2}$
$C_{XY}$	0	$\mu D(L/C)^3 \frac{\epsilon}{(1-\epsilon^2)^2}$
$C_{YX}$	0	0
$C_{YY}$	$\mu D(L/C)^3 \frac{\pi}{2(1-\epsilon^2)^{1.5}}$	$\mu D(L/C)^3 \frac{\pi}{4(1-\epsilon^2)^{1.5}}$
$M_{XX}$	$\rho D(L^3/C) \frac{\alpha \cdot \pi [1-(1-\epsilon^2)^{0.5}]}{12 \epsilon^2 (1-\epsilon^2)^{0.5}}$	$\rho D(L^3/C) \frac{\alpha(i-\pi-2\epsilon)}{24 \epsilon^2}$
$M_{XY}$	0	$\rho D(L^3/C) \frac{\alpha[\ln (1-\epsilon)/(1+\epsilon) -2e]}{24 \epsilon^2}$
$M_{YX}$	0	0
$M_{YY}$	$\rho D(L^3/C) \frac{\alpha \cdot \pi [1-(1-\epsilon^2)^{0.5}]}{12 \epsilon^2}$	$\mu D(L^3/C) \frac{\alpha \cdot \pi [1-(1-\epsilon^2)^{0.5}]}{24 \epsilon^2}$

Where  $i=2 \cdot \cos(-\epsilon)/\sqrt{1-\epsilon^2}$ , and  $\alpha$  ranges from 1.2 to 1.0 for small to moderately large squeeze film Reynolds numbers ( $Re_s = \rho \omega C^2 / \mu$ ). Note that the coefficients  $C_{YX}$  and  $M_{YX}$  are identically zero.

ACKNOWLEDGMENTS

The balance and vibration measurements on the aircraft power turbine used as an example were done by Manuel Marin and Uhn Joo Na. The computer simulations of that example were done by Na. They are graduate students currently working in the Turbomachinery Laboratory at Texas A&M University.

REFERENCES

1. Friedericy, J. A., Eppink, R. T., Liu, Y. N., and Cetiner, A., "An Investigation of the Behavior of Floating Ring Dampers and the Dynamics of Hypercritical Shafts on Flexible Supports," USAAML Technical Report 65-34, UVA Report No. CE-3340-104-65U (1965).
2. Cooper, S., "Preliminary Investigation of Oil Films for the Control of Vibration," Paper 28, Lubrication and Wear Convention, Instn Mech Engrs (1963).
3. Vance, J. M., "Rotordynamics of Turbomachinery," New York, New York: John Wiley and Sons (1988).
4. Gunter, E. J., Jr., Barrett, L. E., and Allaire, P. E., "Design and Application of Squeeze Film Dampers for Turbomachinery Stabilization," *Proceedings of the Fourth Turbomachinery Symposium*, Turbomachinery Laboratory, Texas A&M University, pp. 127-141 (1975).

5. White, D. C., "The Dynamics of a Rigid Rotor Supported on Squeeze Film Bearings," *Proceedings of the Conference on Vibrations in Rotating Systems*, London, pp. 213-229 (1972).
6. Gunter, E. J., Jr., "Rotor-Bearing Stability," *Proceedings of the First Turbomachinery Symposium*, Turbomachinery Laboratory, Texas A&M University, pp. 119-141 (1972).
7. Memmott, E. A., "Tilt Pad Seal and Damper Bearing Applications to High Speed and High Density Centrifugal Compressors," IFToMM, *Proceedings of the 3rd International Conference on Rotordynamics*, Lyon, pp. 585-590 (1990).
8. Memmott, E. A., Letter updating the 1990 numbers of compressors with SFD (1996).
9. Jung, S. Y., San Andres, L., and Vance, J. M., "Measurements of Pressure Distribution and Force Coefficients in a Squeeze Film Damper, Part I: Fully Open Ended Configuration, II: Partially Sealed Configuration," *STLE Tribology Transactions*, 34 (3), pp. 375-389 (1991).
10. Arauz, G. and San Andres, L., "Experimental Study on the Effect of a Circumferential Feeding Groove on the Dynamic Response of a Sealed Squeeze Film Damper," *ASME Paper 95-Trib-50* (1995).
11. Holmes, R. and Sykes, J., "The Effects of Manufacturing Tolerances on the Vibration of Aero-Engine Rotor-Damper Assemblies," Sixth Workshop on Rotor Dynamic Instability Problems in High Performance Turbomachinery, Texas A&M University, College Station, Texas (1990).
12. San Andres, L. and Vance, J. M., "Experimental Measurement of the Dynamic Pressure Distribution in a Squeeze Film Damper Executing Circular Centered Orbits," *ASLE Transactions*, 30 (3), pp. 373-383 (1987).
13. Zeidan, F. Y. and Vance, J. M., "Experimental Investigation of Cavitation Effects on the Squeeze Film Force Coefficients," 1989 ASME Design Technology Conference, Rotating Machinery Dynamics, Montreal, Canada (1989).
14. Roberts, J. B., Holmes, R., and Mason, P. J., "Estimation of Squeeze Film Damping and Inertial Coefficients from Experimental Free-Decay Data," *Proc. of the Instn. of Mechanical Engineers*, 200 (2C), pp. 123-133 (1986).
15. Roberts, J. B. and Ellis, J., "The Determination of Squeeze Film Dynamic Coefficients from Transient Two Dimensional Experimental Data," *ASME Journal of Tribology*, 112, pp. 288-298 (1990).
16. Ramli, M. D., Roberts, J. B., and Ellis, J., "The Determination of Squeeze Film Dynamic Coefficients from Experimental Transient Data," *ASME Journal of Tribology*, 109 (1), pp. 155-163 (1987).
17. Rouch, K. E., "Experimental Evaluation of Squeeze Film Damper Coefficients with Frequency Domain Techniques," *STLE Tribology Transactions*, 33 (1), pp. 67-75 (1990).
18. San Andres, L., "Analysis of Short Squeeze Film Dampers with a Central Groove," *ASME Journal of Tribology*, 114, pp. 659-665 (1992).
19. Arauz, G. and San Andres, L., "Experimental Pressures and Film Forces in a Squeeze Film Damper," *ASME Journal of Tribology*, 115, pp.134-140 (1993).
20. Arauz, G. and San Andres, L., "Effect of a Circumferential Feeding Groove on the Force Response of a Short Squeeze Film Damper," *ASME Journal of Tribology*, 116 (2), pp. 369-377 (1994).

21. Tichy, J. A. and Modest, M., "Squeeze-Film in Arbitrary Shaped Journal Bearings Subject to Oscillations," ASME Journal of Lubrication Technology, *100*, pp. 323-330 (1978).
22. San Andres, L. and Vance, J. M., "Effects of Fluid Inertia and Turbulence on the Force Coefficients for Squeeze Film Dampers," ASME Journal of Engineering for Gas Turbines and Power, *108*, pp. 332-339 (1986).
23. San Andres, L. and Vance, J. M., "Effect of Fluid Inertia on Finite Length Squeeze Film Dampers," ASLE Transactions, *30* (3), pp. 384-393 (1987).
24. San Andres, L. and Vance, J. M., "Force Coefficients for Open-Ended Squeeze Film Dampers Executing Small Amplitude Motions About an Off-Center Equilibrium Position," ASLE Transactions, *30* (1), pp. 69-76 (1987).
25. Vance, J. M. and Kirton, A., "Experimental Measurement of the Dynamic Force Response of a Squeeze Film Bearing Damper," ASME Journal of Engineering for Industry, pp. 1282-1290 (1975).
26. Tichy, J. A., "Measurements of Squeeze Film Bearing Forces to Demonstrate the Effect of Fluid Inertia," ASME Paper 84-GT-11 (1984).
27. San Andres, L., Meng, G., and Vance, J. M., "Experimental Measurement of the Dynamic Pressure and Force Response of a Partially Sealed Squeeze Film Damper," 13th Biennial Conference on Mechanical Vibration and Noise, Miami, Florida, Rotating Machinery and Vehicle Dynamics, ASME Publication, DE-35, pp. 251-256 (1991).
28. San Andres, L., Meng, G., and Yoon, S., "Dynamic Force Response of an Open Ended Squeeze Film Damper," ASME Journal of Engineering for Gas Turbines and Power, *115* (2), pp. 341-343 (1993).
29. Kinsale, I. and Tichy, J., "Numerical and Experimental Study of a Finite Submerged Squeeze Film Damper," Proceedings of the 1989 ASME Vibrations Conference, Machinery Dynamics: Applications and Vibration Control Problems, DE-18 (2) (1989).
30. Zhang, J., Roberts, J. B., and Ellis, J., "Experimental Behavior of Short Cylindrical Squeeze Film Damper Executing Circular Centered Orbits," ASME Journal of Tribology, *116* (3), pp. 528-535 (1994).
31. Zeidan, F. Y. and Vance, J. M., "Cavitation Leading to a Two Phase Fluid in a Squeeze Film Damper," STLE Tribology Transactions, *32*, pp. 100-104 (1989).
32. Zeidan, F. Y. and Vance, J. M., "Cavitation Regimes in Squeeze Film Dampers and Their Effect on the Pressure Distribution," STLE Annual Meeting, Atlanta, Georgia, STLE Pre-print No 89-AM-4B-1 (1989).
33. Zeidan, F. Y. and Vance, J. M., "A Density Correlation for a Two-Phase Lubricant and Its Effect on Pressure Distribution," STLE Tribology Transactions, *33*, pp. 641-647 (1990).
34. Walton, J., Walowitz, F., Zorzi, J., and Schrand, E., "Experimental Observation of Cavitating Squeeze Film Dampers," ASME Journal of Tribology, *109*, pp. 290-295 (1987).
35. Sun, D. C. and Brewe, D., "Two Reference Time Scales for Studying the Dynamic Cavitation of Liquid Films," ASME Journal of Tribology, *114*, pp. 612-615 (1992).
36. Sun, D. C., Brewe, D., and Abel, P., "Simultaneous Pressure Measurements and High Speed Photography Study of Cavitation in Dynamic Loaded Journal Bearings," ASME Journal of Tribology, *115*, pp. 88-95 (1993).
37. Hibner, D. and Bansal, P., "Effect of Fluid Compressibility on Viscous Damper Characteristics," Proceedings of the Conference on the Stability and Dynamic Response of Rotors with Squeeze Film Dampers, Charlottesville, Virginia, pp. 116-132 (1979).
38. Feng, N. S. and Hahn, E. J., "Density and Viscosity Models for Two Phase Homogeneous Hydrodynamic Damper Fluids," ASLE Trans., *29* (3), pp. 361-369 (1986).
39. Mohan, S. and Hahn, E. J., "Design for Squeeze Film Damper Supports for Rigid Rotors," ASME Journal of Engineering for Industry, *96*, pp. 976-982 (1974).
40. Li, X. H. and Taylor, D., "Nonsynchronous Motion of Squeeze Film Damper Systems," ASME Journal of Tribology, *109*, pp. 169-176 (1987).
41. San Andres, L. and Vance, J. M., "Effect of Fluid Inertia on the Performance of Squeeze Film Damper Supported Rotors," ASME Journal of Engineering for Gas Turbines and Power, *110*, pp. 51-57 (1988).
42. Zhao, J. Y., Linnett, I. W., and McLean, L. J., "Unbalanced Response of a Flexible Rotor Supported by a Squeeze Film Damper," ASME Journal of Vibrations and Acoustics, Paper JVA-93-016 (1993).
43. Marmol, R. and Vance, J. M., "Squeeze Film Damper Characteristics for Gas Turbine Engines," ASME Journal of Mechanical Design, *100*, pp. 139-146 (1978).
44. Szeri, A., Raimondi, A., and Giron-Duarte, A., "Linear Force Coefficients for Squeeze Film Dampers," ASME Journal of Lubrication Technology, *105* (3), pp. 326-334 (1983).
45. Leader, M. E., Whalen, J. K., Grey, G. G., and Hess, T. D., Jr., *Proceedings of the Twenty-Fourth Turbomachinery Symposium*, Turbomachinery Laboratory, Texas A&M University, pp. 49-57 (1995).
46. Robison, M., Arauz, G., and San Andres, L., "A Test Rig for the Identification of Rotordynamic Coefficients of Fluid Film Bearings," ASME Turbo Expo'95 Land, Sea and Air Conference, Houston, Texas, ASME Paper 95-GT-431 (1995).
47. San Andres, L., "Theoretical and Experimental Comparisons for Damping Coefficients of a Short Length Open-End Squeeze Film Damper," ASME Turbo Expo'95 Land, Sea and Air Conference, Houston, Texas, ASME Paper 95-GT-98 (1995).
48. Nicholas, J. C., Whalen, J. K., and Franklin, S. D., "Improving Critical Speed Calculations Using Flexible Bearing Support FRF Compliance Data," *Proceedings of the Fifteenth Turbomachinery Symposium*, Turbomachinery Laboratory, Texas A&M University, pp. 69-78 (1986).
49. Murphy, B. T., Manifold, S. M., and Kitzmiller, J. R., "Compulsator Rotordynamics and Suspension Design," Submitted to the 8th EML Symposium, Baltimore, Maryland (1996).
50. Murphy, B. T., "XLROTOR" Rotating Machinery Analysis Inc., Austin, Texas.